5. DESIGN AND TESTING REQUIREMENTS

5.1 SCOPE

This chapter deals with the derivation of design and testing requirements from the measurement, survey and simulation data discussed in the previous chapter. The extraction of fundamental input loading for the definition of the maximum loading limit state, as well as for dynamic finite element analysis, is firstly described.

An approach to establish fatigue equivalent static loading requirements (requiring only static stress analyses but taking fatigue loading into account in a scientific manner), is next presented.

A novel approach, developed by the author, to establish a statistical usage profile (defining both the severity, as well as the magnitude of usage in a fatigue sense, as a probability density function), is described.

The establishment of testing requirements, using both the fatigue equivalent static loading results, as well as the statistical usage profiles, is lastly presented.

As before, the methods are presented as applied to the appropriate case studies.

5.2 FUNDAMENTAL INPUT LOADING

5.2.1 General

In this section, the derivation of fundamental input loading from measured data (for category 1 transducers as defined in paragraph 4.2.5.1) is demonstrated as applied during the bulk tanker case study. Such input loading could be used as input for dynamic finite element analysis, as well as to obtain overload limit state loads.

5.2.2 Maximum Loading Limit State

5.2.2.1 ISO tank container

5.2.2.1.1 Scope

The datalogger recorded accelerations at carefully selected positions on the tank container. From these accelerations maximum loading events were identified. The logger is able to save 256 files that are approximately 1.7 seconds long with a sampling frequency of 602 Hz. The least severe event already recorded is continuously overwritten by more severe events, such that the data recorded at the end of a trip contains the most severe events that the container was subjected to during the measurement period.

The measured acceleration time events were then used as input signals to a mathematical tank container model. From this model the limit state loads (in terms of inertial acceleration [g]) that the tank containers had been subjected to, were determined.

5.2.2.1.2 Dynamic simulation

The measured accelerations at the corner castings serve as input signals for a mathematical model of the tank container. The purpose of the model is to determine the dynamic loads that are transferred between the frame and the tank (vessel) of the container. These loads are expressed in terms of g.

The assumption of an uncoupled six-degree of freedom model (three translational and three rotational degrees of freedom) is made. The model consisted of a mass element that is held into position by spring and damping elements. This is connected to a rigid frame. The measured accelerations are used to excite the frame (refer to Figure 5-1). Two models were used, one with the properties of a full tank container and one that simulated an empty container.

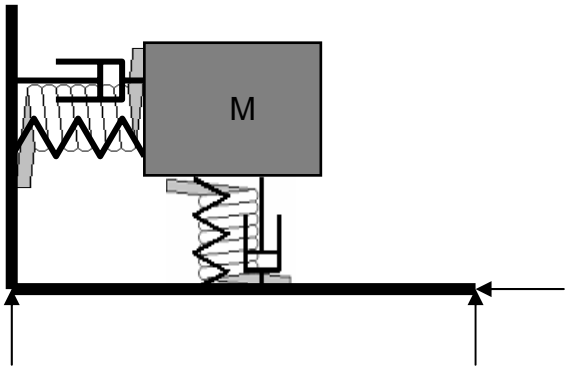

Figure 5-1 Dynamic model of tank container

The dynamic behaviour of the container is described by the equation of motion:

$$[m]\{\ddot{u}\} + [c]\{\dot{u}\} + [k]\{u\} = \{P\}$$

Eq. 5-1

The response was solved by means of the Runge-Kutta method for numerical integration.

From the response the transferred load between the tank and the frame can be calculated by adding the forces at the spring and damping elements. Figure 5-2 shows a typical calculated dynamic loading profile.

5.2.2.1.3 Results

Figure 5-3 shows the maximum amplitude loads, in terms of g, that were calculated for all the full tank container data (the vertical scale is blanks to protect propriety information).

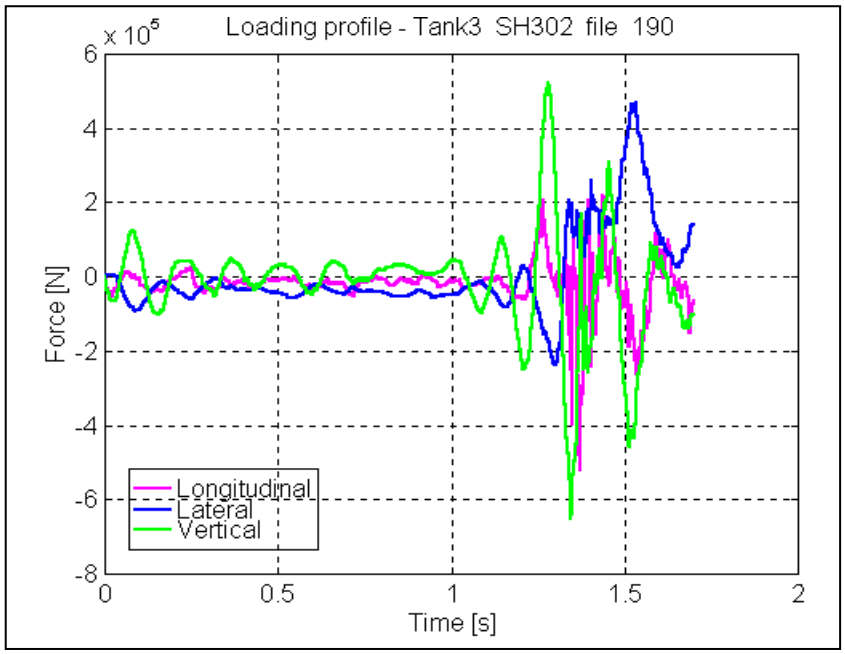

Figure 5-2 Dynamic translational loading profile

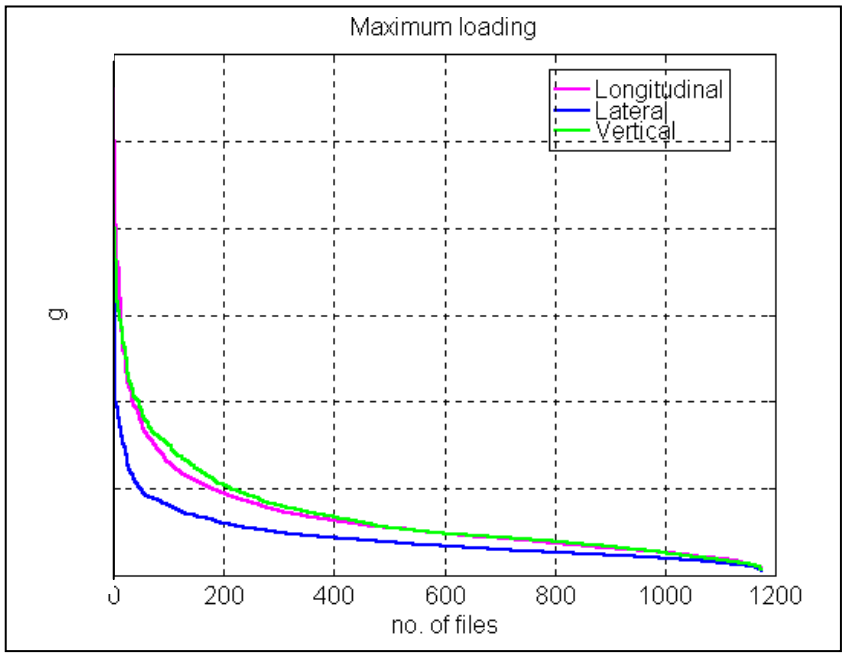

Figure 5-3 Maximum amplitude loads for tank containers

5.2.3 Dynamic Finite Element Analysis

5.2.3.1 General

Measured input loads may be used in a dynamic finite element analysis to calculate stress response.

5.2.3.2 ISO tank container

Figure 5-4 depicts the deformed shape of an ISO tank container at a time instant during a rail road shunting event, using the time domain measured data.

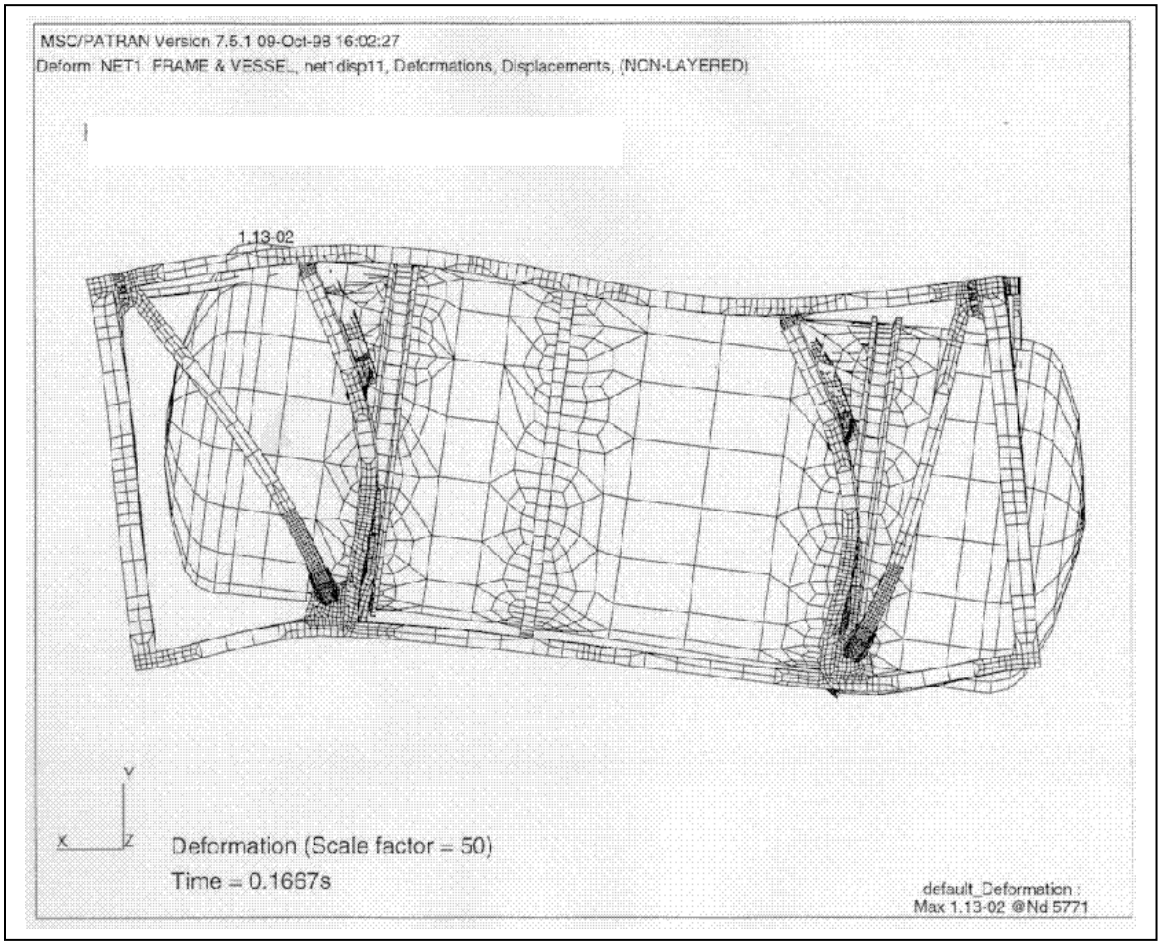

Figure 5-4 Deformed shape of tank container during shunt

The inputs for this dynamic finite element analysis were the measured accelerations on the corner mounts of the tank. Figure 5-5 depicts the correlation between the calculated stress response at a strain gauged position and the directly measured stress during the same event. The benefit of the dynamic finite element analysis method is that stress responses are obtained at all positions on the structure and not only at instrumented positions. The computational effort required is however restrictive. The 4 second event required hours of analysis time.

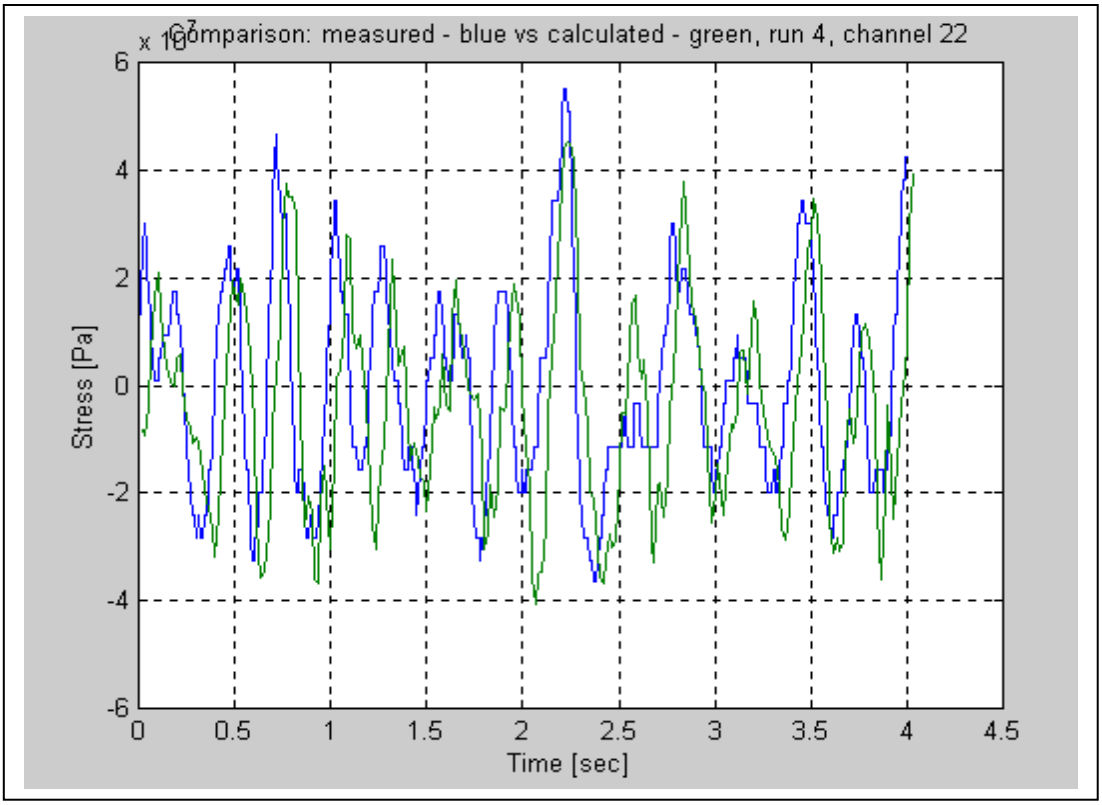

Figure 5-5 Comparison between measured and calculated stresses

5.3 HYBRID MODAL SUPERPOSITION / REMOTE PARAMETER METHOD

5.3.1 General

In paragraph 3.5.8.2.2, the Remote Parameter Analysis (RPA) method, was discussed. The method solves for input loads in the time domain by multiplying measured stresses (remote or indirectly measured parameters) with a transfer matrix between input loads and stresses at the strain gauge positions, which is established through linear-static finite element analysis using unit loads. In the paper by Pountney and Dakin (1992), the method is used to calculate suspension forces, but it could easily be adapted to solve for g-loads, as suggested in paragraph 3.5.8.2.1.

As also suggested in the same paragraph, higher mode response (which could not be described by g-loads), could be taken into account by supplementing the g-load approach with the modal superposition method. The mode-acceleration method discussed in paragraph 3.2.3.4.2 in fact inherently superimposes the quasi-static response with response of excited modes (truncated from the full set of modes).

For the Ladle Transport Vehicle case study, it was required to develop a hybrid methodology, using the RPA method to solve for the quasi-static g-loads, as well as for the modal scaling (participation) factors.

5.3.2 Ladle Transport Vehicle

5.3.2.1 Determination of loading

The measured data (discussed in paragraph 4.2.8) for all the channels were transformed to stresses. For channels 7 and 8, shear stresses were calculated. For the rosette gauge (channels 9,10 & 11), maximum and minimum principal stresses were calculated.

Dynamic loading that could be used together with the finite element model to calculate the dynamic stresses that would cause fatigue, were next derived from the measurement results. For this, the trip 2 data was mainly used, since this trip excluded the test weight event.

Data from channel 3 and 4 (bending gauges on the left and right of the chassis beams) were purposed to derive vertical and lateral loading. The vertical and lateral effects on these 2 channels were decoupled by adding them for vertical and subtracting them for lateral. This is depicted in Figure 5-6. The success of the decoupling can be observed by noticing that the lateral data excludes the effect of the ladle being lifted and put down, whereas the vertical data excludes the effect of turning.

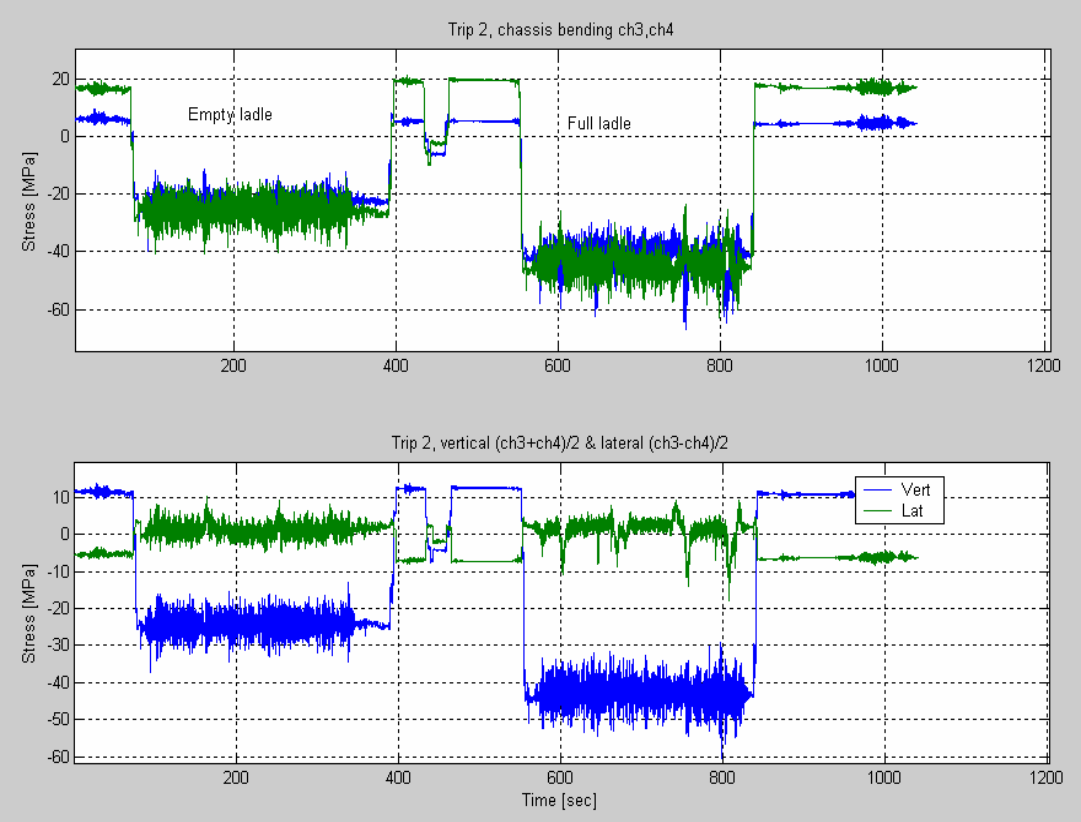

Figure 5-6 Coupled and de-coupled vertical and lateral channels

The frequency content of the channel 3 & 4 data is depicted in Figure 5-7 using a Power Spectral Density plot. Energies at 2.5 Hz, 3.5 Hz and 4.7 Hz were observed. From the decoupled data, it can be seen that the 3.5 Hz frequency belongs to the vertical motion (found to the second natural frequency - vertical bending - of the trailer on its wheels) and the 2.5 Hz frequency belongs to the lateral motion (found to be the first natural frequency – rolling – of the trailer on its wheels).

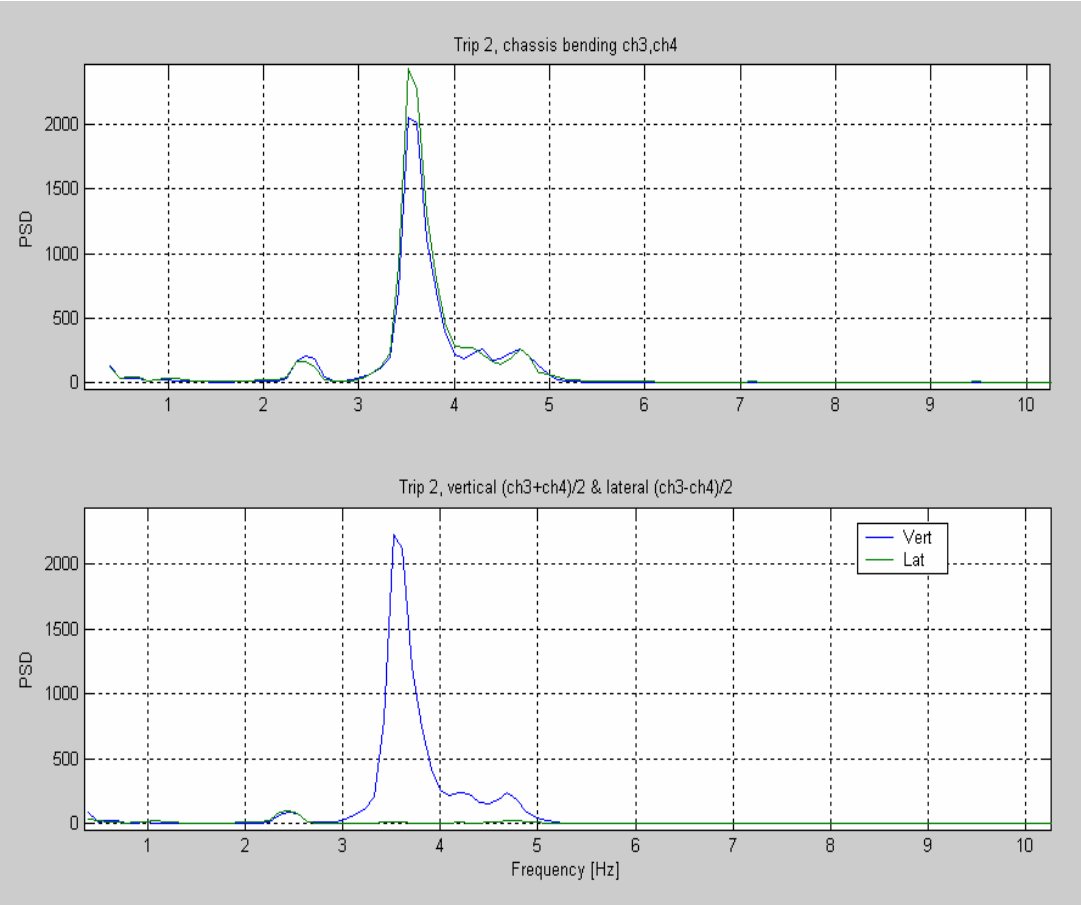

Figure 5-7 Frequency contents of coupled and de-coupled vertical and lateral channels

By also decoupling the data from channels 5 and 6 (crank left and right) and then comparing the vertical data to the vertical data obtained from channels 3 and 4, it was found that it was mostly proportional to each other by a constant factor, which is the same factor determined from the finite element model for pure vertical loading, implying that very little longitudinal loading was present.

The shear gauges (channels 7 & 8) and the rosette gauges (channels 9, 10 & 11), exhibited significant energy at a frequency of 4.7 Hz. This corresponds to the third natural mode, which is a twisting mode of the pillars, with the lid swinging laterally, as depicted in Figure 5-8.

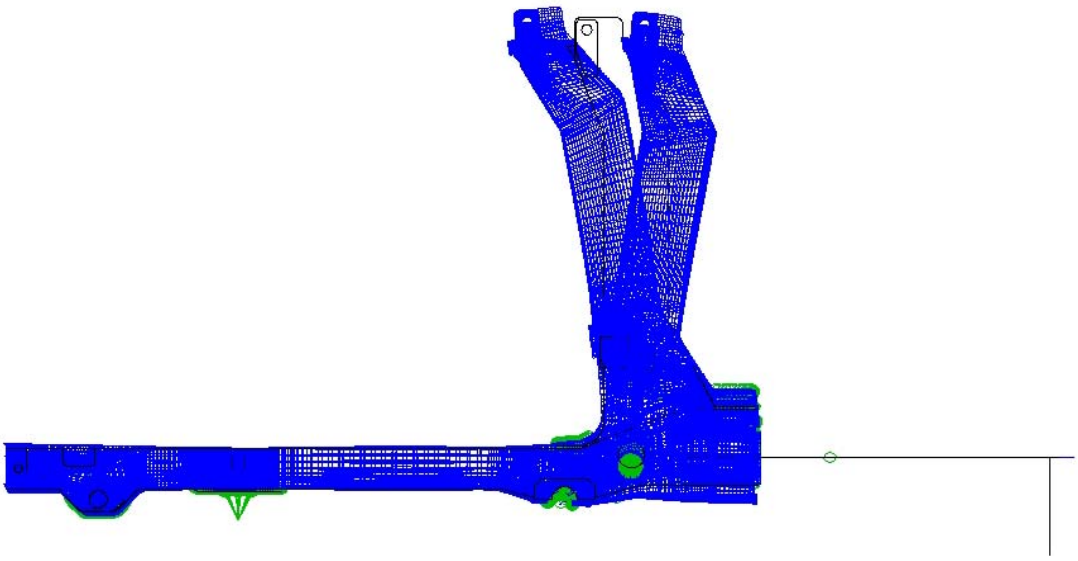

Figure 5-8 Pillar twisting modeshape

This mode cannot be excited if the lid is resting on the ladle, as was the design intent. From the measurements, it was observed that the lid sometimes was resting on the ladle (during trip 1 with a full ladle) and other times not (both trips with the empty ladles and trip 2 with the full ladle). The effect that this had on the strain gauges on the pillars (channels 7 – 11) is depicted in Figure 5-9, showing the significantly lower strains measured on channel 9 during trip 1 with a full ladle, compared to trip 2. The energy at 4.7 Hz during trip 2 and the corresponding reduction of this energy when the lid settles on the ladle during trip 1, can be observed from the frequency plots in Figure 5-10.

Three 'load cases' were therefore identified as having an influence on the dynamic stress/strain response of the structure, namely, vertical loading, lateral loading, as well as the excitation of the third mode shape, if the lid is not resting on the ladle.

The finite element results for these three load cases (unit g loads for the vertical and lateral and modal stresses for the third mode shape) were determined at the various strain gauge positions. The FEA results, as well as the measured results for channels 7 and 8 were identical and therefore only channel 7 was used. The three rosette gauge results were not converted to stress.

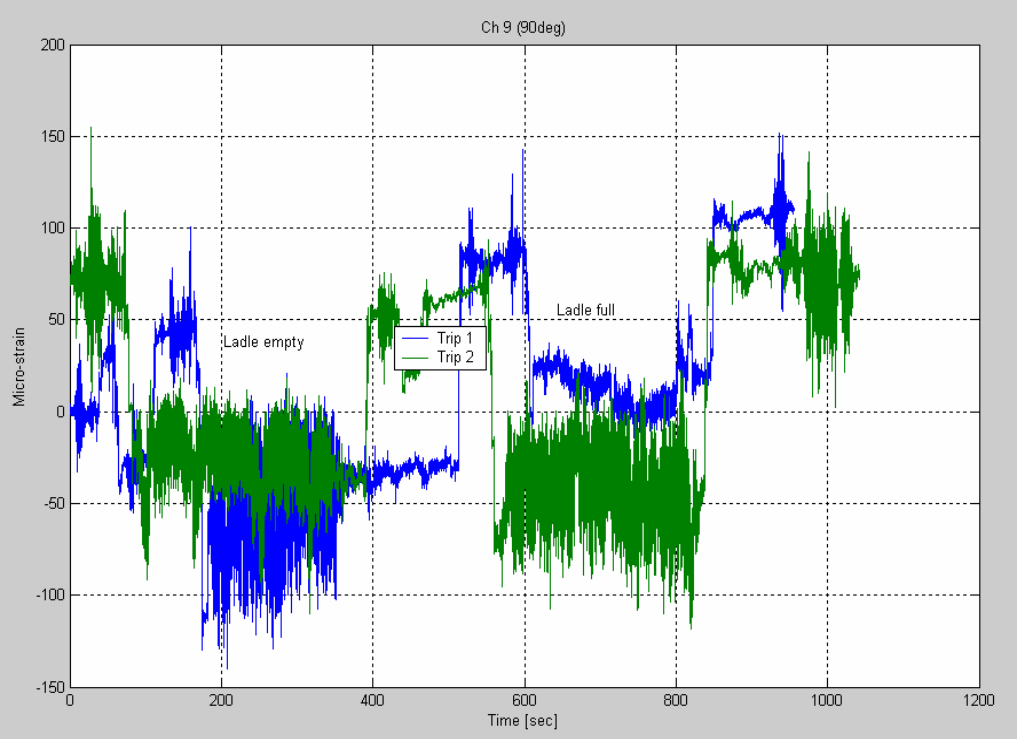

Figure 5-9 Pillar strain gauge for 2 trips

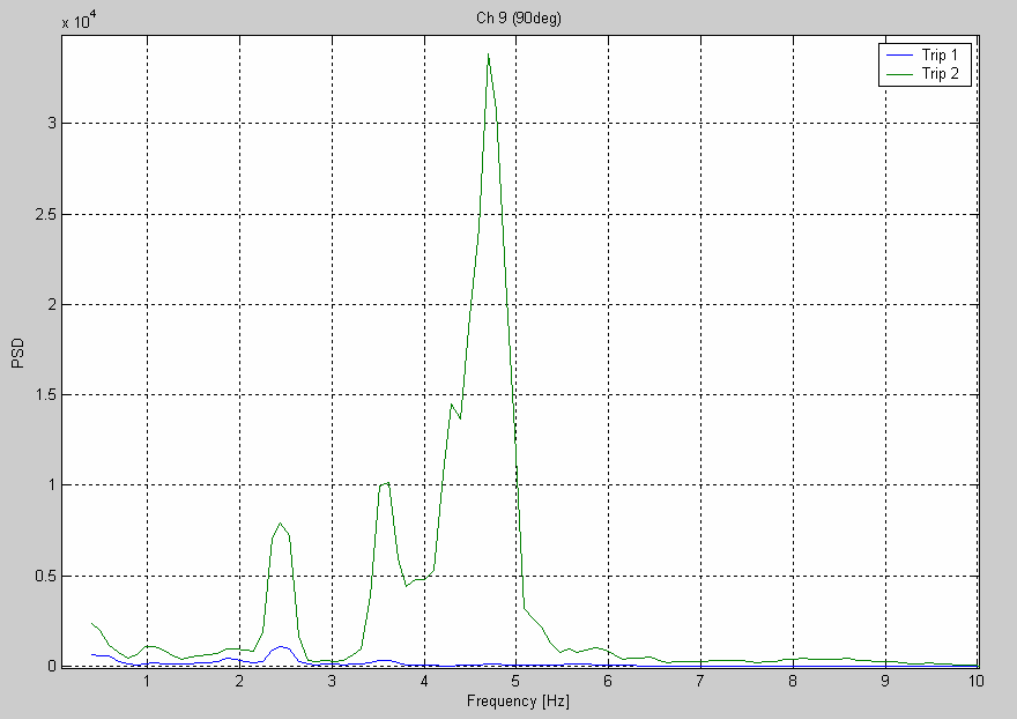

Figure 5-10 Pillar strain gauge frequency content for lid resting and lid not resting

The unit load results were written into the following matrix:

$$[K_{unit\_load\_\sigma\varepsilon}] = \begin{bmatrix} \sigma_{ch3,1gvert} & \sigma_{ch3,1glat} & \sigma_{ch3,modal} \\ \sigma_{ch4,1gvert} & \sigma_{ch4,1glat} & \sigma_{ch4,modal} \\ \sigma_{ch5,1gvert} & \sigma_{ch5,1glat} & \sigma_{ch5,modal} \\ \sigma_{ch6,1gvert} & \sigma_{ch6,1glat} & \sigma_{ch6,modal} \\ \sigma_{ch7,1gvert} & \sigma_{ch7,1glat} & \sigma_{ch7,modal} \\ \varepsilon_{ch9,1gvert} & \varepsilon_{ch9,1glat} & \varepsilon_{ch9,modal} \\ \varepsilon_{ch10,1gvert} & \varepsilon_{ch10,1glat} & \varepsilon_{ch10,modal} \\ \varepsilon_{ch11,1gvert} & \varepsilon_{ch11,1glat} & \varepsilon_{ch11,modal} \end{bmatrix} = \begin{bmatrix} 52.5 & -98 & 0.22 \\ 52.5 & 98 & -0.22 \\ 32 & -36 & -0.2 \\ 32 & 36 & 0.2 \\ 0 & 6 & 0.262 \\ 11.5 & 109 & 10.6 \\ -37.6 & 191 & 9.04 \\ -15.2 & 207 & 5.06 \end{bmatrix} \begin{matrix} MPa \\ MPa \\ MPa \\ MPa \\ MPa \\ \mu\varepsilon \\ \mu\varepsilon \\ \mu\varepsilon \end{matrix}$$

Eq. 5-2

In order to derive the vertical and lateral loads, decoupled channel 3 and 4 results were used, together with the channel 7 results, to solve for the modal contribution. The transfer matrix was therefore calculated as follows:

$$[K_{decoupled}] = \begin{bmatrix} \frac{(\sigma_{ch3,1gvert} + \sigma_{ch4,1gvert})}{2} & \frac{(\sigma_{ch3,1glat} + \sigma_{ch4,1glat})}{2} & \frac{(\sigma_{ch3,modal} + \sigma_{ch4,modal})}{2} \\ \frac{(\sigma_{ch3,1gvert} - \sigma_{ch4,1gvert})}{2} & \frac{(\sigma_{ch3,1glat} - \sigma_{ch4,1glat})}{2} & \frac{(\sigma_{ch3,modal} - \sigma_{ch4,modal})}{2} \\ \sigma_{ch7,1gvert} & \sigma_{ch7,1glat} & \sigma_{ch7,modal} \end{bmatrix}$$

$$[K_{decoupled}] = \begin{bmatrix} 52.5 & 0 & 0 \\ 0 & -98 & -0.22 \\ 0 & 6 & 0.262 \end{bmatrix}$$

Eq. 5-3

The vertical and lateral g-loads, as well as the modal participation factor (all three as time histories), could therefore be solved as follows:

$$[K]\begin{Bmatrix} Vert\_g \\ Lat\_g \\ Modal\_part\_fact \end{Bmatrix} = \{\sigma\}$$

$$[K_{decoupled}]\begin{Bmatrix} Vert\_g(t) \\ Lat\_g(t) \\ Modal\_part\_fact(t) \end{Bmatrix} = \begin{Bmatrix} \frac{(\sigma_{ch3,meas}(t) + \sigma_{ch4,meas}(t))}{2} \\ \frac{(\sigma_{ch3,meas}(t) - \sigma_{ch4,meas}(t))}{2} \\ \sigma_{ch7,meas}(t) \end{Bmatrix}$$

$$\begin{Bmatrix} Vert\_g(t) \\ Lat\_g(t) \\ Modal\_part\_fact(t) \end{Bmatrix} = [K_{decoupled}]^{-1}\begin{Bmatrix} \frac{(\sigma_{ch3,meas}(t) + \sigma_{ch4,meas}(t))}{2} \\ \frac{(\sigma_{ch3,meas}(t) - \sigma_{ch4,meas}(t))}{2} \\ \sigma_{ch7,meas}(t) \end{Bmatrix}$$

Eq. 5-4

This was done for trip 2, which included excitation of the third mode for both the empty and full ladle sections. The results are depicted in Figure 5-11 and Figure 5-12.

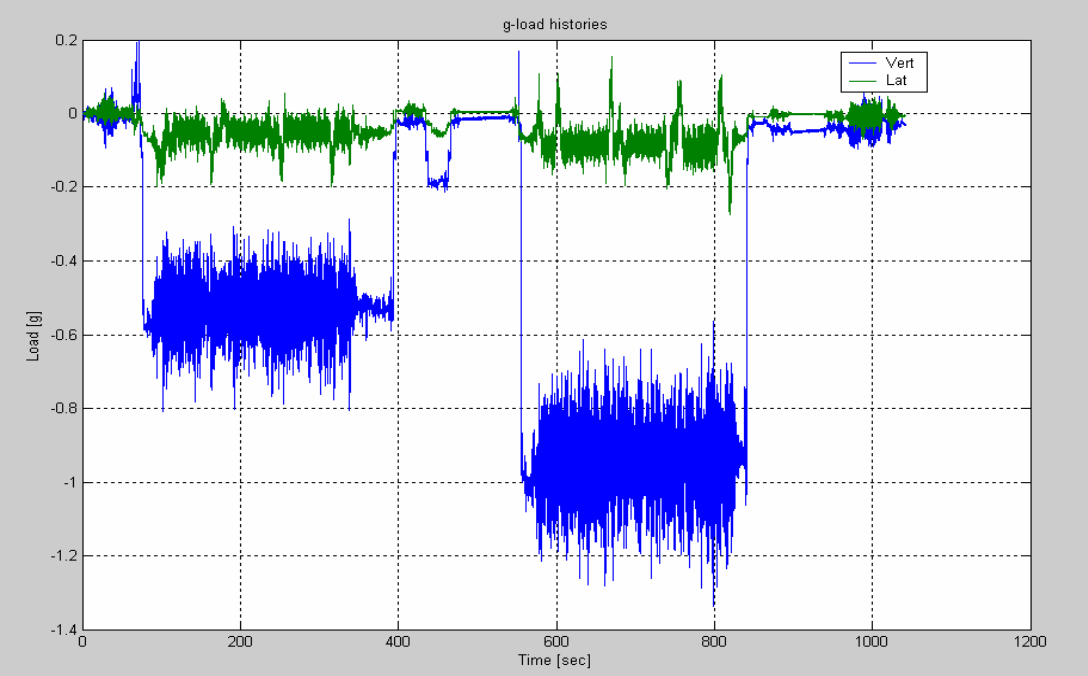

Figure 5-11 Vertical and lateral g-loads

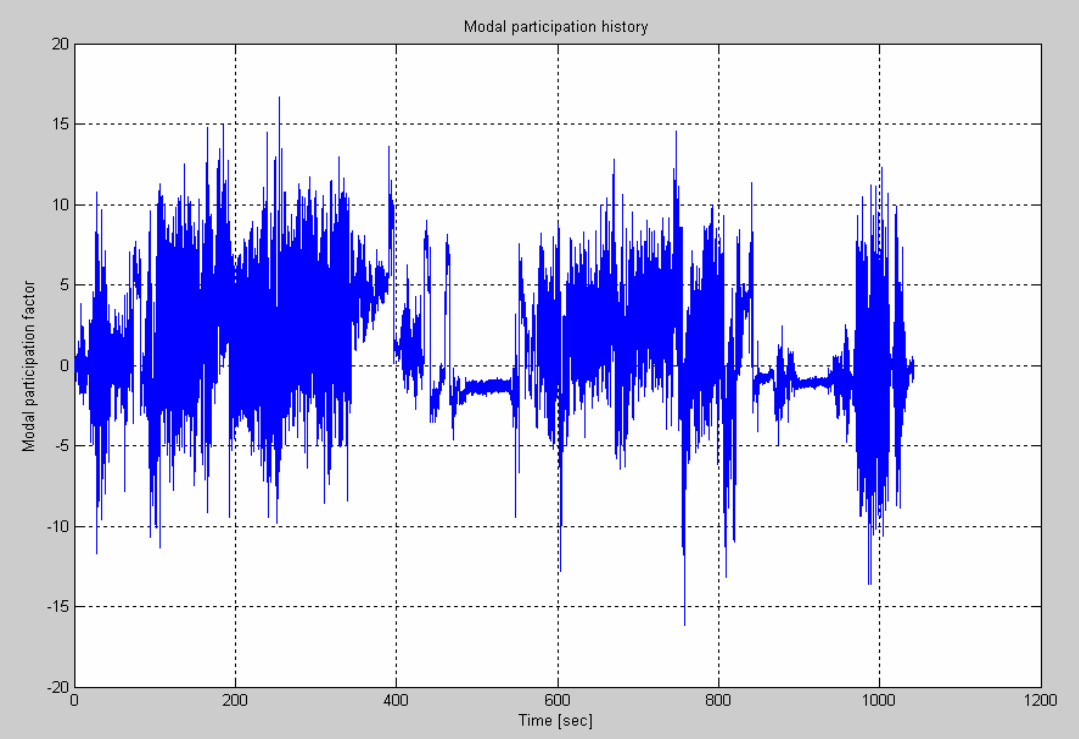

Figure 5-12 Modal participation factor

The loads thus derived could then be used to calculate time histories for all the measured channels, as follows:

$$\begin{Bmatrix} \sigma_3(t) \\ \sigma_4(t) \\ \sigma_5(t) \\ \sigma_6(t) \\ \sigma_7(t) \\ \varepsilon_9(t) \\ \varepsilon_{10}(t) \\ \varepsilon_{11}(t) \end{Bmatrix} = [K_{unit\_load\_\sigma\varepsilon}] \begin{Bmatrix} Vert\_g(t) \\ Lat\_g(t) \\ Modal\_part\_fact(t) \end{Bmatrix}$$

Eq. 5-5

These calculated results may then be compared to the measured time histories. For channels 3, 4 and 7 they are mathematically identical, whereas the success of comparison for the other (redundant) channels gives the confidence that the non-active loads were disregarded and that the results may be used to determine fatigue stresses on the total structure. The comparison is performed by comparing normalized fatigue damages, calculated using the Stress Life method from the measured, as well as the derived time histories. The results are listed in Table 5-1.

Table 5-1 Comparison between measured and calculated normalised damages

	Ch3	Ch4	Ch5	Ch6	Ch7	Ch9	Ch10	Ch11
Measured	97	107	68	77	18	354	483	342
Calculated	97	107	60	60	18	533	471	282

5.4 FATIGUE EQUIVALENT STATIC LOADING

5.4.1 General

Due to the cost of dynamic finite element analyses, as well as the restrictive number of critical positions that can be instrumented for direct fatigue analysis, there is an incentive to simplify the fatigue design process. Such a simplified procedure is also required for design codes, since codes could not stipulate the use of dynamic finite element analysis methods, or measurements, since this would restrict their usage to only sophisticated users, as well as requiring the availability of an existing structure for measurements.

In many industries, design codes or less formal design criteria are used where allowance for fatigue is simply made by prescribing higher than limit state design loads and/or incorporating safety factors on the allowable stresses. The origin and applicability of such criteria are often uncertain.

In the following paragraph, a methodology for deriving fatigue equivalent static criteria for fatigue design, is proposed.

5.4.2 Methodology

5.4.2.1 Uni-axial axis method

Using measured data, a fatigue design criterion can be developed that requires only static finite element analysis. In the case of heavy vehicles, the vertical bending stress (measured for example on the vehicle chassis) can be used, due to the fact that it is assumed that the vertical induced loads would represent most of the fatigue damage experienced on a vehicle structure.

5.4.2.1.1 Measurements

In the derivation below, a transport vehicle (considered to be typical in terms of weight, suspension etc. of all vehicles in its class) is assumed to have been instrumented with strain gauges on its main chassis beams, measuring vertical bending stresses. The vehicle is assumed to have been driven on roads representative of normal usage for a distance of 200 km whilst measurements were taken.

5.4.2.1.2 Measured damage calculation

The measured stress-time histories are cycle-counted, to yield a spectrum of stress ranges ($\Delta\sigma_i$) and number of counted cycles (n_i). A relative fatigue damage (relative because generic material properties, b and S_f are used) can be calculated using the stress-life approach. The exponent (b) of the stress-life equation is chosen as –0.33, being the gradient of almost all of the SN-curves in fatigue design codes (ECCS (1985), BS 8118 (1991)), whilst the coefficient S_f is arbitrary, since it will cancel out in the calculation.

Firstly, the number of cycles to failure at each stress range can be calculated with the reverse of Eq. 3-14:

$$N_i = \left(\frac{\Delta\sigma_i}{S_f} \right)^{1/b} \qquad \textbf{Eq. 5-6}$$

Then the total damage is calculated using Miner's damage accumulation theory (Eq. 3-21):

$$\text{Damage} = \sum \frac{n_i}{N_i} = \sum \frac{n_i}{\left(\frac{\Delta\sigma_i}{S_f}\right)^{1/b}} \qquad \textbf{Eq. 5-7}$$

5.4.2.1.3 Equivalent stress range calculation

The purpose then would be to obtain an equivalent bending stress range which would, when repeated an arbitrary (n_e) times, cause the same damage to the beam to what would be caused during the total life (e.g. 1 million km) of the vehicle, made out of repetitions of the measured trip.

This damage could be calculated as follows:

$$N_e = \left(\frac{\Delta\sigma_e}{S_f}\right)^{1/b}$$

$$\text{Damage}_e = \frac{n_e}{N_e} = \frac{n_e}{\left(\frac{\Delta\sigma_e}{S_f}\right)^{1/b}} \qquad \textbf{Eq. 5-8}$$

$\Delta\sigma_e$ can be solved by equating:

$$\text{Damage}_e = \text{Damage} \times 1 \text{ million km} / 200 \text{ km} \qquad \textbf{Eq. 5-9}$$

Therefore, combining Eq. 5-7, Eq. 5-8 and Eq. 5-9:

$$\sum \frac{n_i}{\left(\frac{\Delta\sigma_i}{S_f}\right)^{1/b}} = \frac{n_e}{\left(\frac{\Delta\sigma_e}{S_f}\right)^{1/b}}$$

$$\Delta\sigma_e = \left(\sum \frac{\Delta\sigma_i{}^m n_i}{n_e}\right)^{1/m} \qquad \textbf{Eq. 5-10}$$

With n_e=2 million

m= $-1/b$=3

n_i=cycles counted for each stress range from the total measured trip, multiplied by 1million/200

The arbitrary choice of n_e = 2 million was done because the fatigue classifications in the ECCS code are denoted by the stress range values in MPa at 2 million cycles, for each SN-curve.

5.4.2.1.4 Fatigue equivalent static loading calculation

The bending stress (σ_{1g}), caused by 1 g (unit) vertical inertial loading at the strain gauge position, is then calculated using finite element analysis.

The fatigue equivalent static loading (FESL), is then calculated as follows:

$$FESL = \frac{\Delta\sigma_e}{\sigma_{1g}}$$

Eq. 5-11

This load is a single axis (vertical), inertial load range (i.e. peak-to-peak), measured in [g], which, when applied 2 million times, would represent the fatigue loading of 1 million kilometres.

5.4.2.1.5 Life assessment

The FESL is then applied on the finite element model in a static analysis. The stresses thus calculated are interpreted as stress ranges, which would be repeated 2 million times during the life of 1 million kilometres. The fatigue life at each critical position may then be calculated, using the appropriate SN-curve relevant to the detail at each position.

The fatigue damage calculated at the strain gauge position (using the same SN-curve as for the measured damage calculation) would be equal to the measured damage, due to Eq. 5-9. It is then assumed that the operational dynamic stress responses at any other position on the structure, are proportional to the dynamic stress at the strain gauge position by the same constant factor as the ratio between the vertical-static-inertial-load stress responses at the other positions and the strain gauge position. If this is the case, the fatigue damages calculated at the other positions would be the same as what would have been calculated from measured dynamic stresses at those positions.

In the application of the FESL method, it would therefore be good practice to place redundant (not used for FESL calculation) strain gauges on the structure. The measurements from the redundant gauges may then be used to calculate fatigue damages that may be compared to those calculated using the FESL. Close correlation would imply a high confidence level in the validity of the assumptions made. The placement and number of redundant gauges are important and are demonstrated in paragraph 5.2.2.1.3.

5.4.2.2 Multi-axial loading method

In certain cases, the assumption that the contribution of loads other than vertical to fatigue damage may be neglected, cannot be made. Sedan vehicles are mostly used on well surfaced roads, but are cornering and braking more frequently and more severely than heavier vehicles, implying that longitudinal and lateral loads should be considered. Tank containers are subjected to severe longitudinal loading during rail shunting operations. Heavy vehicles with high centres-of-gravity may exhibit relatively high frequency and magnitude rocking response, implying lateral loading.

The single axis method described in the previous paragraphs may easily be adapted to take into account multi-axial loading. The vehicle chassis, used as an example in the single axis method derivation, will again be employed, but the assumption is now made that vertical, longitudinal, as well as lateral inertial loading, are to be considered.

5.4.2.2.1 Measurements

To be able to solve three FESLs, three non-redundant strain gauge channels are required. The correct placement of these gauges is non-trivial. Three bending gauges

next to each other on one of the chassis beams would obviously measure the same for any of the three loads and could therefore not be used to solve three unknown loads.

In this idealised example, three bending gauges are placed as depicted in Figure 5-13, representing a chassis frame, the four wheel positions, as well as two cross beams. The chassis would be loaded by inertial loads on some mass connected to the chassis beams at various places and is supported at the wheel positions. Channels 1 and 3 would respond the same for vertical and longitudinal loads, but differently for a lateral load, whereas channel 2 would respond differently to all three loads to the other two channels. Measurements are recorded on a typical route as before.

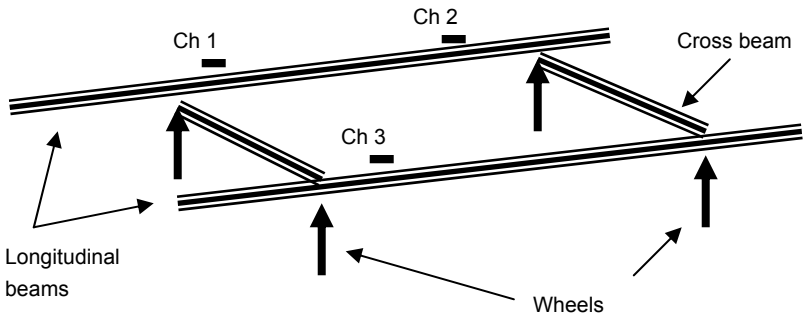

Figure 5-13 Idealised chassis with strain gauges

5.4.2.2.2 Measured damage calculation

As described in paragraph 5.4.2.1.2 above, rainflow cycle counting is performed on the data of all three channels, yielding σ_i and n_i results for all three.

5.4.2.2.3 Equivalent stress range calculation

Employing again Eq. 5-10, the equivalent stress range ($\Delta\sigma_{e,chj}$) for each channel (j) is calculated:

$$\Delta\sigma_{e,chj} = \left(\sum \frac{\Delta\sigma_i{}^m n_i}{n_e} \right)^{1/m}$$

5.4.2.2.4 Fatigue equivalent static loading calculation

The finite element model is loaded with separate unit inertial loads in the three directions and the stress responses ($\sigma_{load,chj}$) at each of the strain gauge positions and for each load, are determined. The stress response (σ_{chj}) at the three gauge positions due to a combined inertial load case would then be:

$$\begin{bmatrix} \sigma_{vert,ch1} & \sigma_{long,ch1} & \sigma_{lat,ch1} \\ \sigma_{vert,ch2} & \sigma_{long,ch2} & \sigma_{lat,ch2} \\ \sigma_{vert,ch3} & \sigma_{long,ch3} & \sigma_{lat,ch3} \end{bmatrix} \begin{Bmatrix} g_{vert} \\ g_{long} \\ g_{lat} \end{Bmatrix} = \begin{Bmatrix} \sigma_{ch1} \\ \sigma_{ch2} \\ \sigma_{ch3} \end{Bmatrix}$$

Eq. 5-12

Rearranging Eq. 5-12 and substituting the equivalent stress range results, enable the calculation of the FESL in three directions:

$$FESL = \begin{Bmatrix} \Delta g_{vert} \\ \Delta g_{long} \\ \Delta g_{lat} \end{Bmatrix} = \begin{bmatrix} \sigma_{vert,ch1} & \sigma_{long,ch1} & \sigma_{lat,ch1} \\ \sigma_{vert,ch2} & \sigma_{long,ch2} & \sigma_{lat,ch2} \\ \sigma_{vert,ch3} & \sigma_{long,ch3} & \sigma_{lat,ch3} \end{bmatrix}^{-1} \begin{Bmatrix} \Delta\sigma_{e,ch1} \\ \Delta\sigma_{e,ch2} \\ \Delta\sigma_{e,ch3} \end{Bmatrix}$$

Eq. 5-13

The above equation may be generalised for any number of inertial or non-inertial loads $\{L_{i=1\ to\ a}\}$, requiring (a) measurement channels to solve (a) fatigue factors $\{FF_{i=1\ to\ a}\}$, for every load:

$$FESL = \begin{Bmatrix} FF_1 \\ : \\ FF_a \end{Bmatrix} = \begin{bmatrix} \sigma_{1,ch1} & .. & \sigma_{a,ch1} \\ : & :: & : \\ \sigma_{1,cha} & .. & \sigma_{a,cha} \end{bmatrix}^{-1} \begin{Bmatrix} \Delta\sigma_{e,ch1} \\ : \\ \Delta\sigma_{e,cha} \end{Bmatrix}$$

Eq. 5-14

5.4.2.2.5 Life assessment

The calculated loads are applied simultaneously to the finite element model. The stresses thus calculated again may be interpreted as stress ranges to be applied 2 million times during a 1 million kilometre life. Using the appropriate SN-curves for each critical position, the fatigue life of the total structure may be calculated.

5.4.3 Comparison with Remote Parameter Analysis Method

The uni-axial FESL method would yield exactly the same results as the uni-axial RPA method, with the only difference being that the cycle counting is performed directly on the single measurement signal, thereafter using Fatigue Equivalent Static loads and stresses, instead of calculating load and stress, time histories first and then performing cycle counting on all critical stress histories. The FESL method therefore improves on the RPA method by being less computationally intensive.

A further important improvement is achieved due to the fact that the FESL method results in a single, design independent load requirement, which could be used in design codes.

The multi-axial FESL method achieves the same advantages over the multi-axial RPA method, but does not yield the same life prediction results on the total structure. This discrepancy is due to the fact that phase information is lost after the conversion of the multi-axial time histories to Fatigue Equivalent Static Loads.

If the idealised chassis example depicted in Figure 5-13 was subjected to exactly in-phase (or 180° out-of-phase) sine wave inertial loading in the vertical and lateral directions (with no longitudinal load), each load causing the same amplitude of stresses at channels 1 and 3, the measured result would be double the amplitude on one of the channels and zero amplitude on the other, resulting in the latter channel having a zero $\Delta\sigma_e$. The σ_{1g} results would be the same in absolute magnitude for both channels and both loads, but would be of the same sign for the vertical loading and of opposite signs for the lateral loading. The FESL result would then be correctly calculated, resulting in $\Delta g_{vert} = \Delta g_{lat}$.

If, however, the vertical and lateral loads are randomly out-of-phase, as would normally be the case, the FESL calculation may often result in $\Delta\sigma_{e,ch1}$ being approximately equal to $\Delta\sigma_{e,ch3}$, since the combined vertical and lateral loading would statistically cause similar stress responses on both chassis rails. In this case, the solution of Δg_{vert} and Δg_{lat} would be ill-conditioned. If the vertical and lateral loading were decoupled before cycle counting, by adding the two channels for vertical loading and subtracting them for lateral loading, 'more correct' results for Δg_{vert} and Δg_{lat} would be achieved, but application of these loads in a static finite element analysis would yield an overestimated damage on the one rail (where the two loads, now implicitly in-phase, are superimposed) and an underestimated damage on the other (where the loads would out-of-phase).

5.4.4 Fuel Tanker

5.4.4.1 Finite element analysis

Detailed finite element half models were constructed of the front and rear trailers, employing mainly shell elements. 1 g vertical inertial loading was applied. The liquid load was simulated using pressure loading. The front trailer model and results are depicted in Figure 5-14 and Figure 5-15.

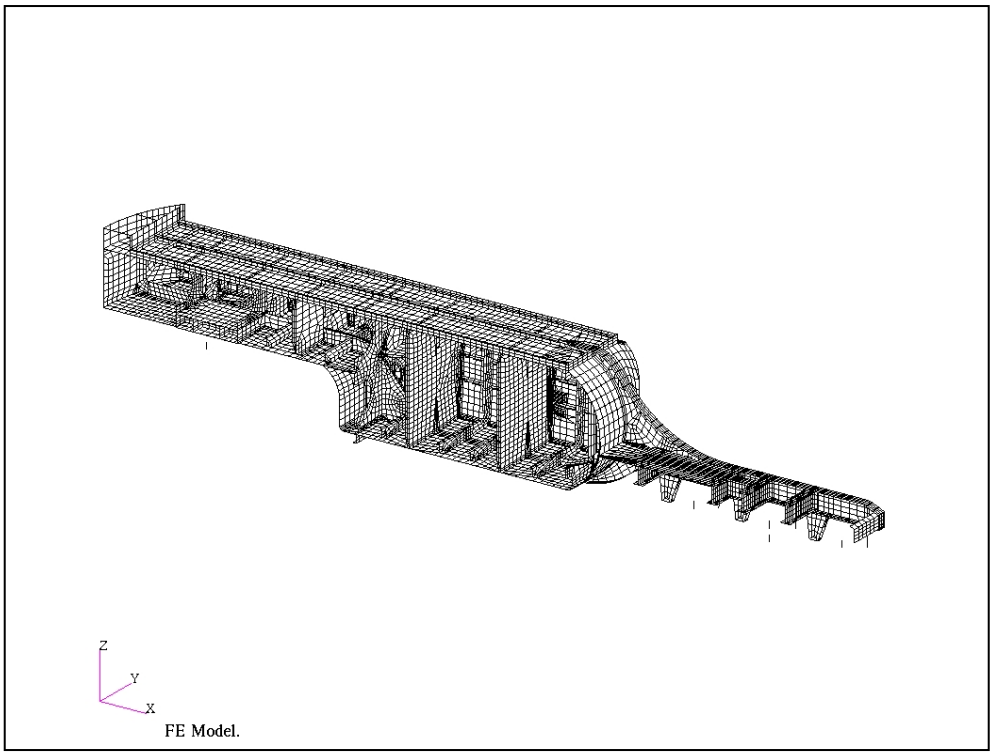

Figure 5-14 Finite element model of fuel tanker front trailer

5.4.4.2 Measured damage calculation

Fatigue damage calculations were performed on the measured data, using the process depicted in Figure 3-11. A fatigue exponent of b=-0.333 was used.

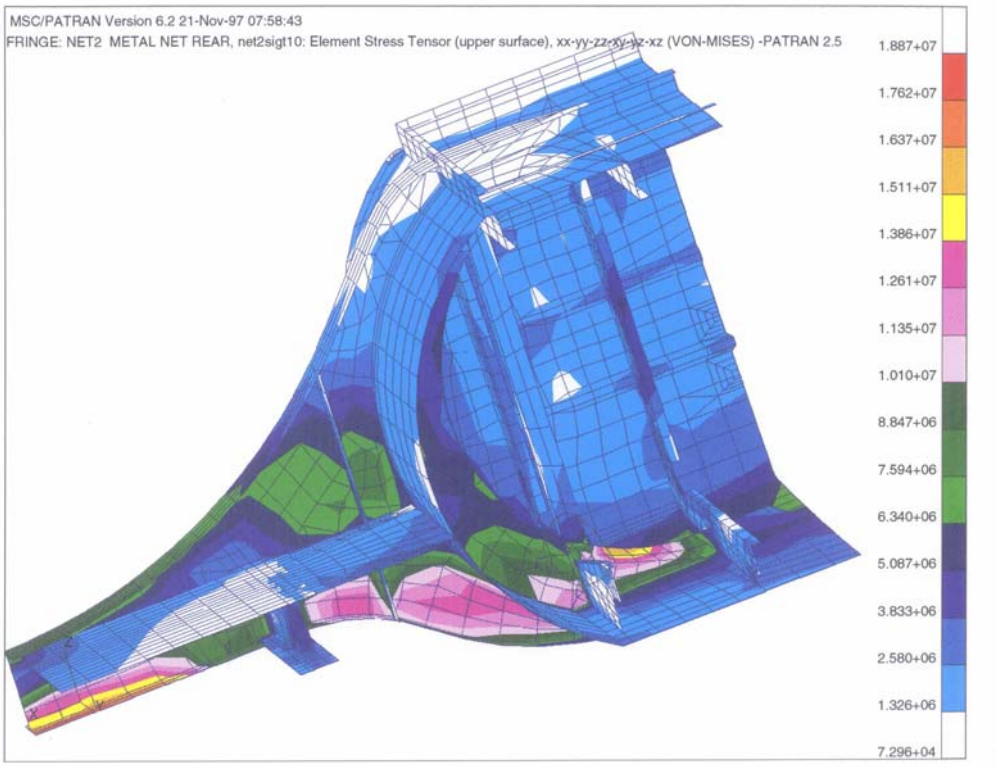

Figure 5-15 Finite element results on fuel tanker front trailer

5.4.4.3 Fatigue equivalent static load calculation

The bending stress measured by channel 34 on the front trailer chassis was used for the FESL calculation, due to the fact that it is again assumed that the vertically induced loads would represent most of the fatigue damage experienced on the vehicle structure. An equivalent stress range corresponding to 2 million cycles (arbitrarily chosen to correspond to the number of cycles at which the weld class is specified), was calculated which would cause the same damage to what was caused at that channel during the total measured trip extrapolated to a life distance of 2 million kilometres (the fact that the life distance is equal to the chosen cycles is coincidental). Eq. 5-10 was again used for this purpose with: N=2 million, m=3 and n_i=cycles counted for each stress range full the total trip, multiplied by 2 million/distance travelled during measurements.

This was done on the assumption that a life of 2 million kilometres would be expected of these vehicles.

The resultant equivalent stress range was found to be 15.5 MPa. The stress calculated by FEA for a 2 g load was 50 MPa. The equivalent vertical load therefore corresponds to a vertical acceleration of 15.5/50 x 2 g = 0.62 g. It is then implied that any stress calculated in the vehicle structure at 0.62 g vertical loading would be repeated 2 million times during a life of 2 million kilometres. All welds should then be of a class higher than the nominal stress at the weld calculated for 0.62 g loading. According to BS 8118 (1991), the class for a fillet weld would be 20 and for a butt weld 24.

5.4.5 ISO Tank Container

5.4.5.1 Scope

In this section, the processing of the fatigue domain data is described. The purpose of the processing is to determine fatigue loading criteria for the analysis or testing of tank containers. The multi-axial method derived in paragraph 5.4.2.2, was used.

5.4.5.2 Measured data and fatigue processing

A total of approximately 1100 days of data was processed. This included data received from 4 tank containers. The rainflow counting process was performed onboard of the datalogger in real time.

Due to a constraint in the datalogger design, the resolution of the stress ranges counted, together with the corresponding number of cycles, had to be fixed for all channels and all files. All stress ranges between 0 and 24 MPa (first bin) were counted as the same, and so were ranges between 24 and 48 MPa (second bin) and so forth up to 31 bins. For the less sensitive channels and files where the stresses were low, this implied that, if the maximum stress range was less than e.g. 48 MPa, only two bins of counting resulted. A method to improve the resolution after the fact, had to be devised, since it would be inaccurate to assume all counted cycles in e.g. the first bin were 24 MPa large (many smaller cycles would then be overestimated)

5.4.5.3 Improvement of cycle counting resolution

When a log-log plot is made of originally counted cycles vs ranges for well populated channels and files, it was found that the relationship is always linear (which is to be expected from a statistical point of view). This may be observed in Figure 5-16.

A mathematical process was therefore implemented, which repopulated all counting results, by enforcing a linear relationship between cycles and stress ranges on a log-log scale, with the maximum stress range being upper value of the highest bin for which cycles were counted and assumed then to be one cycle and the lowest range being the filter cut-off range of 3.7 MPa and at the same time enforcing the total number of cycles to be the same as the original count.

The results of such an exercise are depicted in Figure 5-17 (original count only in 2 bins) and Figure 5-18 (improved resolution result).

5.4.5.4 Equivalent stress range

The counting results (table of stress range-$\Delta\sigma_i$ and cycles-n_i) for each channel and file are used to calculate a fatigue damage, using Eq. 3-14 and Eq. 3-21:

$$\Delta\sigma = S_f N^b$$

$$S_f = \text{fatigue coefficient}$$

$$b = \text{fatigue exponent}$$

$$D_{ch} = \sum \frac{n_i}{N_i}$$

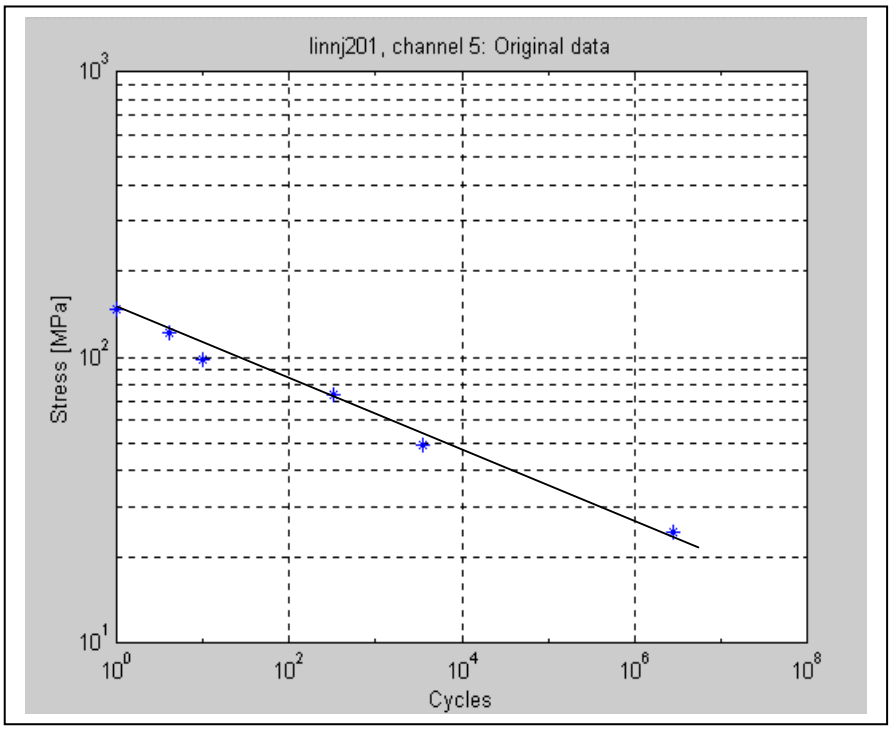

Figure 5-16 Log-log linearity between cycles and stress ranges

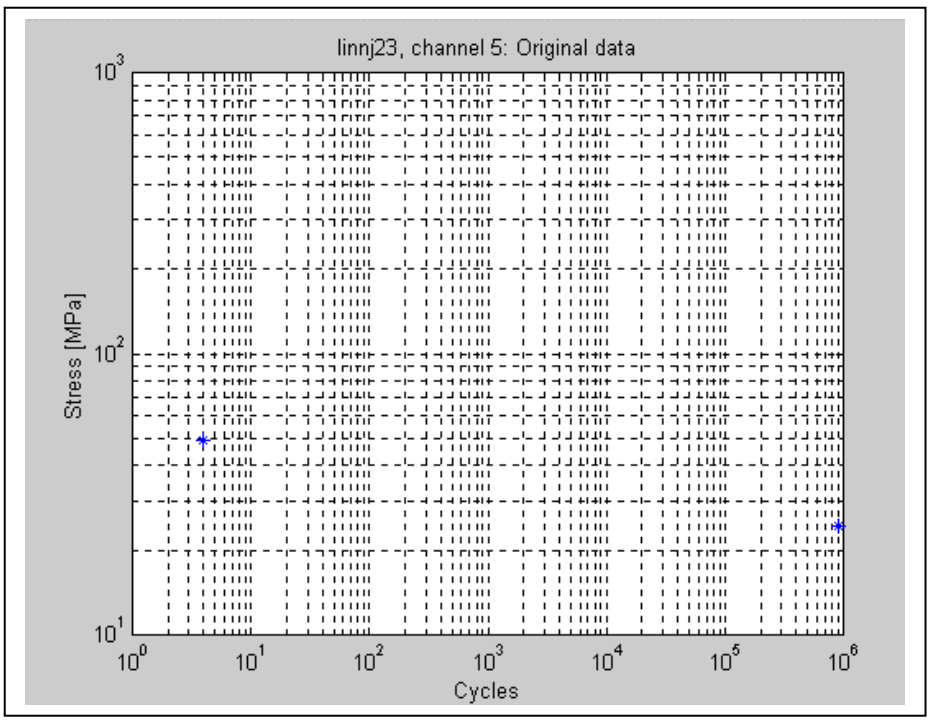

Figure 5-17 Data before improvement of resolution

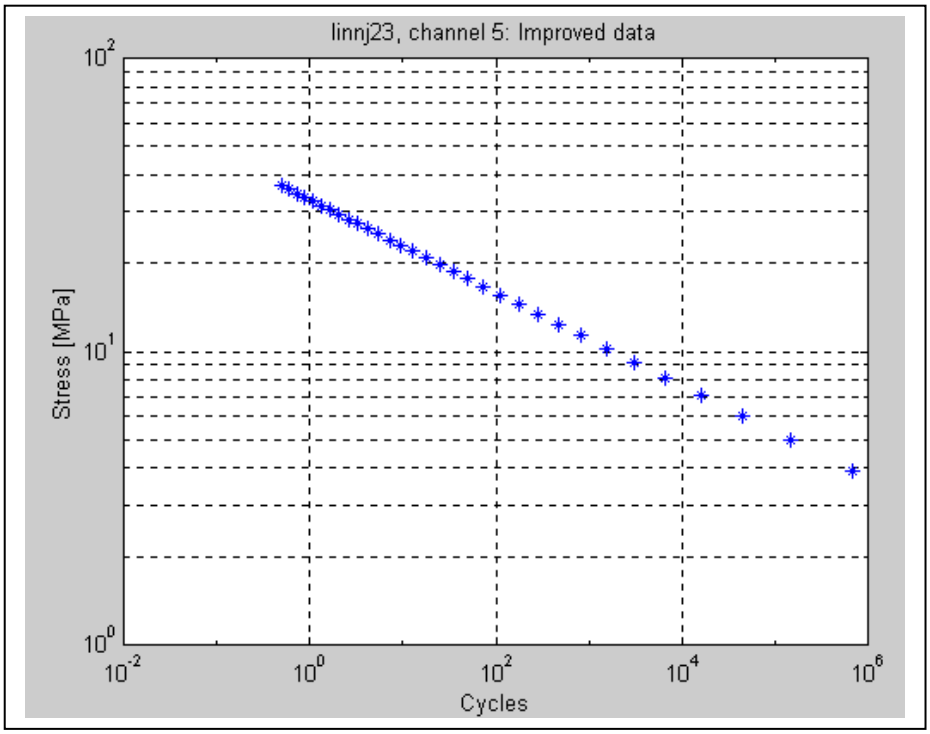

Figure 5-18 Data after improvement of resolution

The material property S_f is arbitrarily chosen (it cancels out later) and b is chosen as –0.33 (for welds). The damages are accumulated per channel for each file (a file typically representing 6 weeks of measurements). The damages per channel are then normalised ($D_{n,ch}$) to a damage per ten years of operation, by dividing it by the total accumulated measurement duration and multiplying it with the number of days in 10 years.

An equivalent constant amplitude stress range is calculated for each channel, which would cause the same damage as the normalised damage, if the range is applied an arbitrary 2 million times. This is achieved through the inverse of the above equations:

$$\Delta\sigma_{e,ch} = S_f \left(\frac{2 \times 10^6}{D_{n,ch}} \right)^b$$

Eq. 5-15

Each channel would then have an equivalent stress range, which would, if applied 2 million times, give the same damage as what was measured (extrapolated to 10 years).

5.4.5.5 Finite element analysis

Originally, pitching loading was not included as a load case. The result was that a longitudinal load was calculated that was higher than the vertical load. The high longitudinal result was explained by the fact that pitching of the tank when loaded with out of phase vertical loading back and front, would have a longitudinal influence. The high centre of gravity of the tank on a vehicle would imply that out of phase vertical loading would result in significant longitudinal effect, even though this would not translate in heavy loading onto the longitudinal bearing structures. It was decided to add a

pitching load (a positive inertial load on one end and an equal but negative load on the other), which would therefore be applied in combination with a lower longitudinal load that would then be calculated if the pitching effect was subtracted.

It is then required to determine the combination of g-loading (vertical, longitudinal, lateral and pitching) that would give this stress at the different strain gauge positions. For this, a finite element analysis was performed (model depicted in Figure 5-19). 1 g loading was applied on a full tank in each direction (L_i) separately and the stress results [$\sigma_{Li,ch}$] at the different strain gauge positions noted for each load case. For the pitching load the analysis was performed where the one end of the container was fixed and the other accelerated by 1 g.

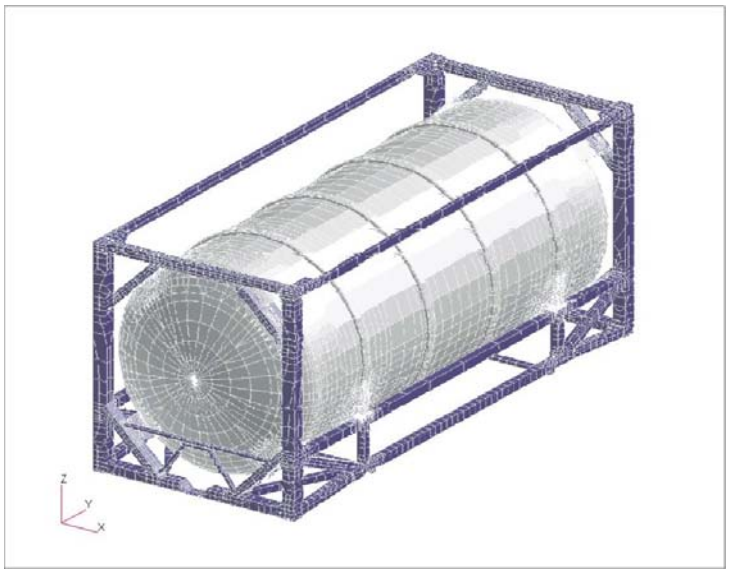

Figure 5-19 Finite element model of tank container

5.4.5.6 Fatigue equivalent static load calculation

The unit load FEA results are used as the elements in the transfer matrix of Eq. 5-14. The equivalent g-loading ranges are then determined by solving Eq. 5-14, with (a=4):

$$FESL = \begin{Bmatrix} FF_1 \\ : \\ FF_a \end{Bmatrix} = \begin{bmatrix} \sigma_{1,ch1} & .. & \sigma_{a,ch1} \\ : & :: & : \\ \sigma_{1,cha} & .. & \sigma_{a,cha} \end{bmatrix}^{-1} \begin{Bmatrix} \Delta\sigma_{e,ch1} \\ : \\ \Delta\sigma_{e,cha} \end{Bmatrix}$$

$$FESL = \begin{Bmatrix} \Delta g_{e,vert} \\ \Delta g_{e,long} \\ \Delta g_{e,lat} \\ \Delta g_{e,pitch} \end{Bmatrix} = \begin{bmatrix} \sigma_{vert,ch1} & \sigma_{long,ch1} & \sigma_{lat,ch1} & \sigma_{pitch,ch1} \\ \sigma_{vert,ch2} & \sigma_{long,ch2} & \sigma_{lat,ch2} & \sigma_{pitch,ch2} \\ \sigma_{vert,ch3} & \sigma_{long,ch3} & \sigma_{lat,ch3} & \sigma_{pitch,ch3} \\ \sigma_{vert,ch4} & \sigma_{long,ch4} & \sigma_{lat,ch4} & \sigma_{pitch,ch4} \end{bmatrix}^{-1} \begin{Bmatrix} \Delta\sigma_{e,ch1} \\ \Delta\sigma_{e,ch2} \\ \Delta\sigma_{e,ch3} \\ \Delta\sigma_{e,ch4} \end{Bmatrix}$$

Eq. 5-16

The fatigue equivalent static g-loads thus determined may then be used as a fatigue loading criterion (apply the g-loads 2 million times to simulate a 10 year life).

Since seven channels were available and only four unknown loads required solving, it was possible to produce several answers, using any four of the seven channels to give a 4x4 transfer matrix. There are 35 different such combinations, as listed below:

Permutations of 4 channels chosen from 7 =

1	1	1	1	1	1	1	1	1	1	1	1	1	1	1	1
2	2	2	2	2	2	2	2	2	2	3	3	3	3	3	3
3	3	3	3	4	4	4	5	5	6	4	4	4	5	5	6
4	5	6	7	5	6	7	6	7	7	5	6	7	6	7	7

1	1	1	1	2	2	2	2	2	2	2	2	2	2	3	3
4	4	4	5	3	3	3	3	3	3	4	4	4	5	4	4
5	5	6	6	4	4	4	5	5	6	5	5	6	6	5	5
6	7	7	7	5	6	7	6	7	7	6	7	7	7	6	7

3	3	4
4	5	5
6	6	6
7	7	7

The solutions thus obtained are depicted in Figure 5-20 below. The coloured stars represent the results for each of the 35 combinations for each of the four loads. Each load should be interpreted separately, but they are plotted using the same vertical scale, with zero g being at the origin of the graph. The vertical scale is blanked out to protect propriety information. Normal distributions (depicted in blue), were fitted to the 35 results for each load, exhibiting relatively narrow spreads around the four mean values of each distribution ($\Delta g_e(ver)_{me}$, $\Delta g_e(lon)_{me}$, $\Delta g_e(lat)_{me}$, $\Delta g_e(pit)_{me}$). The green line depicted on the graph merely connects the mean values of each load, showing the relative magnitudes of the loads.

It was decided to use these mean values of each load in order to minimise the differences across the 35 solution sets. The stability of the results across the 35 sets implies that the mean solution, applied as loads to the finite element model, would cause stresses approximately equal to the measurements based fatigue equivalent stresses at all of the seven measurement positions.

This in turn implies that, given that the seven measurement positions are representative of the total structural response, the fatigue equivalent static loads obtained through the above process, may be employed to accurately determine the fatigue life of the total structure.

The importance of the concept of placing redundant strain gauges is hereby demonstrated. Since the results are defined in terms of inertial loads, it is possible to use the results for any design.

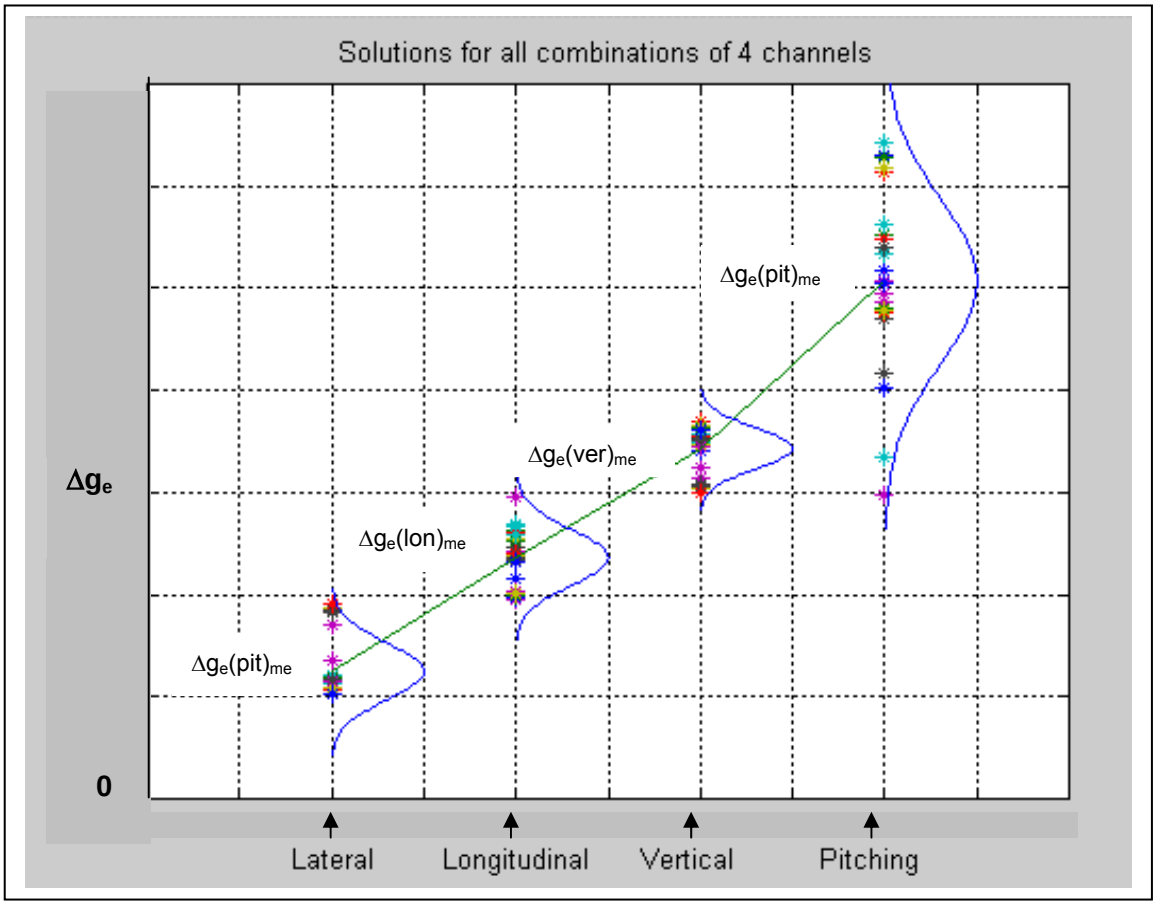

Figure 5-20 FESL solutions for different combinations of measurement chs

5.4.6 Load Haul Dumper

5.4.6.1 Finite element analysis

5.4.6.1.1 Model

The geometry and mesh of the vehicle structure were generated in MSC Patran. The model is depicted in Figure 5-21. The rear chassis and boom section of the vehicle was modelled. The front chassis was simulated in the model with rigid elements to ensure that the force transfer was correct.

5.4.6.1.2 Constraints and loads

The model was constrained at the rear wheel axle in the vertical (Y) and lateral (Z) directions to simulate the rear suspension. The model was constrained at the front axle in all three translations and rotation about the longitudinal axis.

The masses of the engine, bucket and front chassis were introduced to model as mass elements with the appropriate centre of gravity positions and masses. Three load cases, each implying a different model, were considered:

- Model A where the bucket is empty, the boom is resting on its stops and inertial loading is applied to simulate empty travelling.
- Model B where the bucket is full (6 000 kg), the boom is resting on its stops and inertial loading is applied to simulate full travelling.
- Model C where the boom is lifted and loading is applied on the boom to simulate the effect of forces on the bucket during loading or off-loading.

5.4.6.1.3 Quasi-static comparison with measurements

The finite element analysis was done for three conditions, with certain masses and loads, as described in paragraph 5.4.6.1.2. It is then possible to compare the static trends obtained from the stress results against the measured results.

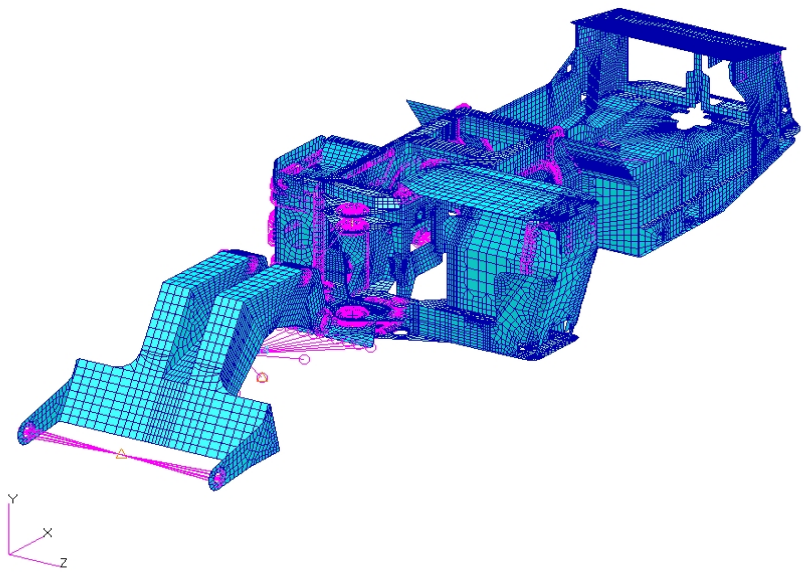

Figure 5-21 Finite element model

The first step in this comparison is to identify the periods in the measurement duration during which the vehicle was travelling empty or full, as well as when the bucket was lifted, to correspond with the three models. This was done by identifying the bucket position using pictures taken during the test by the real-time camera. These photos had a time stamp on and can be directly related to the measured signals. A channel that is

sensitive to bucket loads was selected and the finite element stresses at the location of that strain gauge for all three models were used to construct a quasi-static time history, corresponding to the measured events. This would not take the dynamic effects into account. The measured stress at channel 7 and the predicted stress according to FEA are depicted in Figure 5-22. The blue curve in Figure 5-22 corresponds to a bucket load of 5 tons. The trends of the stresses correlate well.

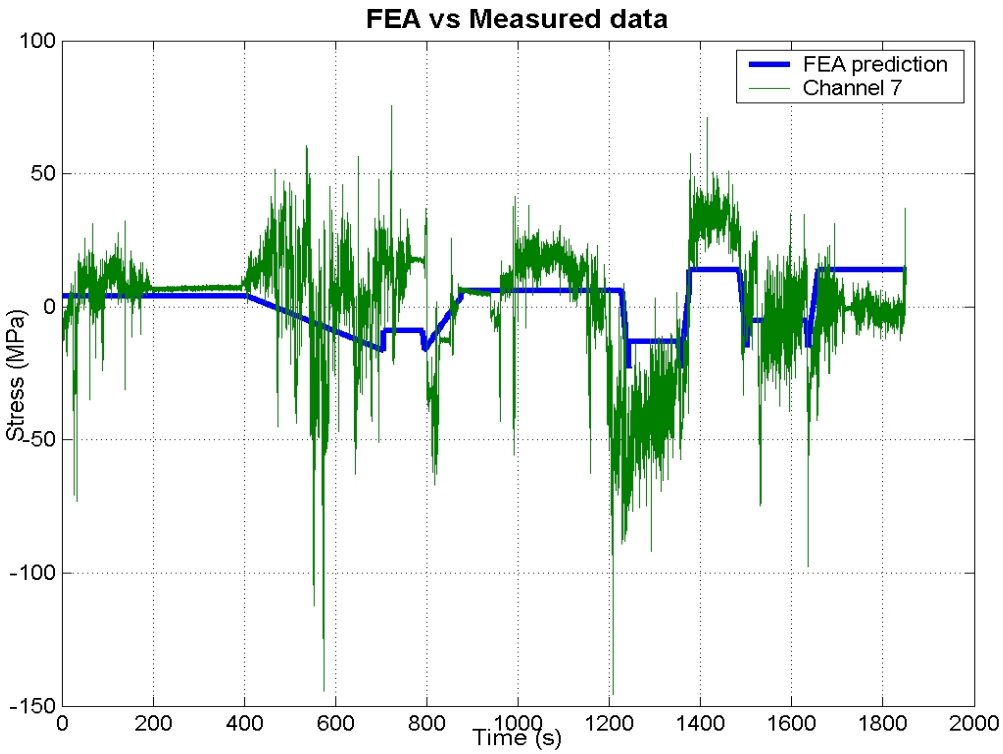

Figure 5-22 Quasi-static FEA vs measurements

5.4.6.1.4 Unit load analysis

It was decided to apply only vertical loading for all three models, since vertical loads would by far represent the largest proportion of fatigue damaging loads on the vehicle structure (horizontal loads due to hitting the side walls, ramming the bucket into a pile, braking, turning and accelerating, would occur far less frequently than vertical loads). Three strain gauges were therefore chosen in order to solve for the fatigue equivalent static loads (all vertical) for the three models, namely channel numbers 3, 4 and 7. The finite element stress results at each gauge position for 1 g load applied to each model were as follows:

$$\begin{bmatrix} \sigma_{1g,A3} & \sigma_{1g,B3} & \sigma_{1gC3} \\ \sigma_{1g,A4} & \sigma_{1g,B4} & \sigma_{1g,C4} \\ \sigma_{1g,A7} & \sigma_{1g,B7} & \sigma_{1g,C7} \end{bmatrix} = \begin{bmatrix} -3.5 & -12.5 & -12.5 \\ 12 & 12 & 4.34 \\ 5.8 & 25 & 35 \end{bmatrix} \text{MPa}$$

Eq. 5-17

5.4.6.2 Measured damage calculation

Relative fatigue damages for the measured runs for each of the three chosen channels were calculated. These damages (D_3, D_4, D_7) were calculated after performing Rainflow cycle counting (providing n_i and $\Delta\sigma_i$), using Eq. 5-7:

$$D_j = \sum \frac{n_i}{N_i} = \sum \frac{n_i}{\left(\frac{\Delta\sigma_i}{S_f}\right)^{1/b}}$$

$$\text{with } b = -0.33 \text{ as before}$$

$$S_f = \text{arbitrary}$$

Eq. 5-18

The calculated damages were extrapolated to total damages for a 10 000 hour life as follows:

$$TD_j = D_j \times 10\,000 \text{ hours / duration of measurement run (in hours)}$$

5.4.6.3 Fatigue equivalent static load calculation

The process that was followed in this case study to calculate fatigue equivalent static loads, differed from the single-axis (vertical loading only) methodology described in paragraph 5.4.2.1 in that three finite element models contributed to the total damage. The process was based on summation of damages, since the damages induced in the structure due to stresses on the three different models, are uncoupled (occur in separate durations).

For model (k) and strain gauge position (j), the damage (D_{kj}) induced by stresses (unit load stress (σ_{kj}) for model (k) at gauge (j) from Eq. 5-17, multiplied by the to-be-determined fatigue equivalent static load ($FESL_k$)), may be calculated using Eq. 5-8:

$$D_{kj} = \frac{n}{\left(\frac{\sigma_{kj} \times FESL_k}{S_f}\right)^{1/b}}$$

$$\text{with } b = -0.33 \text{ as before}$$

$$S_f = \text{same as in Eq. 5 - 27}$$

$$n = 2 \text{ million (chosen value)}$$

Eq. 5-19

The total damage at gauge position (j) must then be equal to the summation of the damages (D_{kj}) for k = A, B, C:

$$\frac{2\times10^6}{\left(\frac{FESL_A\sigma_{Aj}}{S_f}\right)^{-3}} + \frac{2\times10^6}{\left(\frac{FESL_B\sigma_{Bj}}{S_f}\right)^{-3}} + \frac{2\times10^6}{\left(\frac{FESL_C\sigma_{Cj}}{S_f}\right)^{-3}} = TD_j$$

Eq. 5-20

Three such equations exist, for each of the three channels (j = 3, 4, 7). From these three equations, the three unknown fatigue equivalent static loads could be solved as ($FESL_A$ = 4.2 g, $FESL_B$ = 1.1 g, $FESL_C$ = 1.85 g). When the above loads are applied to the three models, the stresses that are calculated are then used as stress ranges, applied 2 million times in a 10 000 hour life, and by using the appropriate SN-curves, damages at any critical position may be calculated by adding the damages for the three models, as depicted in Figure 5-23.

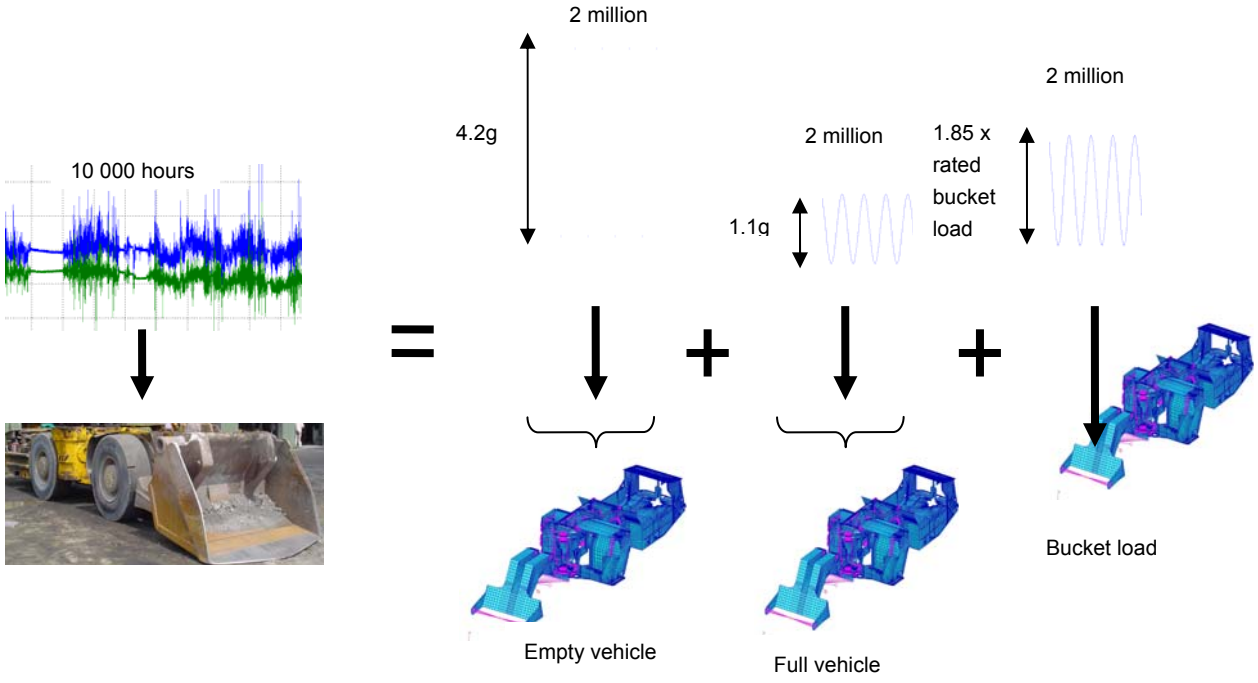

Figure 5-23 Equivalent fatigue loading

5.5 STATISTICAL MODEL

5.5.1 General

As was previously discussed, it is expected that several parameters defining the usage profile of a vehicle are not deterministic. Methods to establish a statistical model for usage profiles are dealt with in this section, using the light commercial vehicles as case studies.

5.5.2 Methodology

The methodology entails the following basic steps:

- Questionnaire exercise (dealt with in paragraph 4.2.7)
- Measurements (dealt with in paragraph 4.2)
- Fatigue processing of measurement data.
- Fitting probability density functions on parameters.

5.5.3 Minibus

5.5.3.1 Fatigue calculations

5.5.3.1.1 Method

The measured data obtained from the strain gauge bridge applied to the left torsion bar was employed to calculate relative damages induced on each route and road category. Sample calculations were performed on the other torsion bar data. It was observed that the damage ratios between different roads based on the left and right torsion bars were equivalent.

The measured data was organized in different files, each consisting of a certain category of road (categorized according to the questionnaire data), on the computer.

The measured strains were converted to stresses by assuming that the relationship between stress and strain was linear elastic. The range-pair-range algorithm was employed to count the fatigue cycles contained in the measured signals. The stress life criterion, together with the Miner damage accumulation law were employed to calculate the relative damage for each measurement file. An assumed SN curve with a gradient of b = -0.33 was employed.

The damage for each file was divided by the distance represented by the file, to obtain a damage/km for each terrain type.

5.5.3.1.2 Results

The damage/km results for files in each category were averaged to yield an average relative damage/km for each category. These results are listed in Table 5-2.

Table 5-2 Damage results per category

Category	Description	Average relative damage per kilometre
1	Highway	1.81×10^{-4}
2	Secondary tar	7.38×10^{-4}
3	Smooth gravel	2.53×10^{-3}
4	Rough gravel	3.16×10^{-3}
5	Very rough	3.78×10^{-3}

The relative damage per kilometre induced by the sequence measured on the durability track was calculated as 1.16×10^{-2}.

5.5.3.2 Statistical processing of questionnaire data

Based on the measurements that had been performed, it was attempted to calculate a relative damage per kilometre for every questionnaire participant. It was not possible to accurately distinguish between the damage caused by central town, suburban and country

roads and it was therefore decided to unite these three categories into one category, namely, secondary tar roads.

Table 5-2 lists the different categories that were used, together with the average relative damage per kilometre as obtained from the measurement results.

The average relative damage per kilometre for each participant was subsequently calculated as follows:

$$D_{average}/km = \sum_{category=1}^{5}\left(D_{average}/km_{category} \times \frac{percentage_{category}}{100} \right)$$

Eq. 5-21

A lognormal probability density function (PDF) was then fitted to these results:

$$f(x_1) = \frac{1}{x_1 \sigma_y \sqrt{2\pi}} e^{-\frac{1}{2}\left(\frac{\ln x_1 - \mu_y}{\sigma_y}\right)^2}$$

$$\text{with } x_1 = D/km$$

$$y = \ln x_1, \text{being normally distributed (mean} = \mu_y, \text{variance} = \sigma_y^2)$$

Eq. 5-22

The fitted curve together with the raw data histogram is shown in Figure 5-24. It may be observed that a good fit was achieved. A similar procedure was followed to obtain an expression for the statistical distribution of the km/day data:

$$f(x_2) = \frac{1}{x_2 \sigma_y \sqrt{2\pi}} e^{-\frac{1}{2}\left(\frac{\ln x_2 - \mu_y}{\sigma_y}\right)^2}$$

$$\text{with } x_2 = km/day$$

$$y = \ln x_2, \text{being normally distributed (mean} = \mu_y, \text{variance} = \sigma_y^2)$$

Eq. 5-23

The achieved fit is shown in Figure 5-25. Again a good fit was achieved.

It was however expected that the variables (D/km and km/day) would not be statistically independent. A participant logging high kilometres per day probably would primarily be using highways, implying low D/km. Statistical theory states that if two dependent variables can separately be fitted to lognormal distributions, then a bivariate lognormal PDF may be employed to obtain a two-dimensional distribution, defined by Eq. 5-24.

A 2-D plot of this function is shown in Figure 5-26.

$$f(x1,x2) = \frac{1}{x_1\, x_2\, \sigma_{y_1}\, \sigma_{y_2}\, 2\pi \sqrt{1-\rho^2}}\, e^{z}$$

$$\text{with } z = -\frac{1}{2(1-\rho^2)}\left[\left(\frac{\ln x_1 - \mu_{y_1}}{\sigma_{y_1}}\right)^2 - 2\rho\left(\frac{\ln x_1 - \mu_{y_1}}{\sigma_{y_1}}\right)\left(\frac{\ln x_2 - \mu_{y_2}}{\sigma_{y_2}}\right) + \left(\frac{\ln x_2 - \mu_{y_2}}{\sigma_{y_2}}\right)^2\right]$$

$$\rho = \frac{\sigma_{y_{12}}}{\sigma_{y_1}\sigma_{y_2}} \qquad \textbf{Eq. 5-24}$$

$$x_1 = \text{D/km}$$

$$x_2 = \text{km/day}$$

$$y_1 = \ln x_1, \text{being normally distributed (mean} = \mu_{y_1}, \text{variance} = \sigma^2_{y_1})$$

$$y_2 = \ln x_2, \text{being normally distributed (mean} = \mu_{y_2}, \text{variance} = \sigma^2_{y_2})$$

By definition:

$$\int_0^\infty \int_0^\infty f(x_1, x_2)\, dx_1\, dx_2 = 1$$

Eq. 5-25

Having thus achieved an excellent mathematical description of the D/km and km/day distributions pertaining to minibus taxi operators, it would be possible to extract durability requirements according to any company target (e.g. one year warranty for 90 % of the buyers, or 300 000 km for 90 % of the buyers). The process to extract durability requirements from these distributions is described later.

The results obtained thus far, however, have been based solely on theoretical exercises (fatigue calculations, questionnaires and statistical processing). In order to acquire sufficient confidence in these results, it was required to, in some way, verify the theoretical results. Such verification was subsequently attempted, based on the failure data that was available on a gearbox mounting crossmember of the vehicle. This verification firstly involved laboratory testing of the crossmembers, which is described in the next chapter.

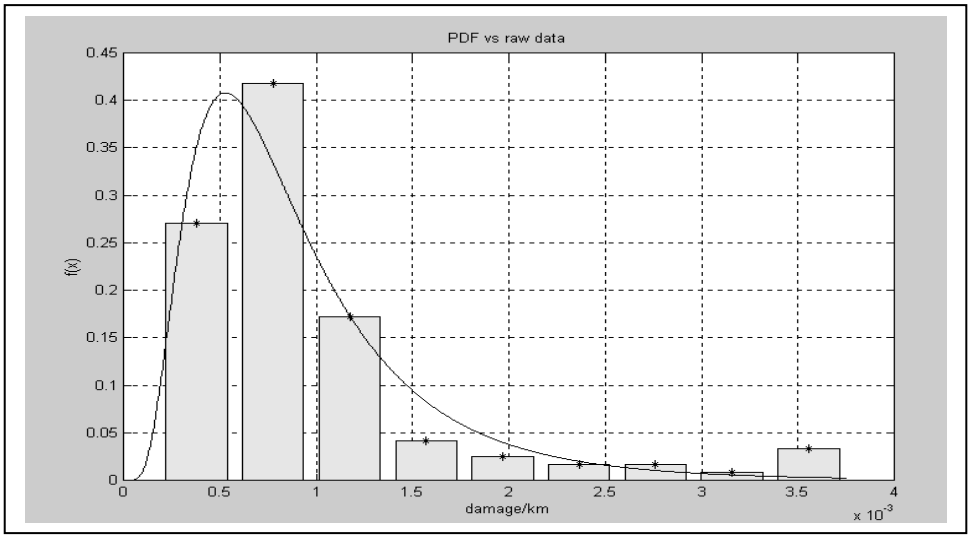

Figure 5-24 PDF of D/km versus raw data

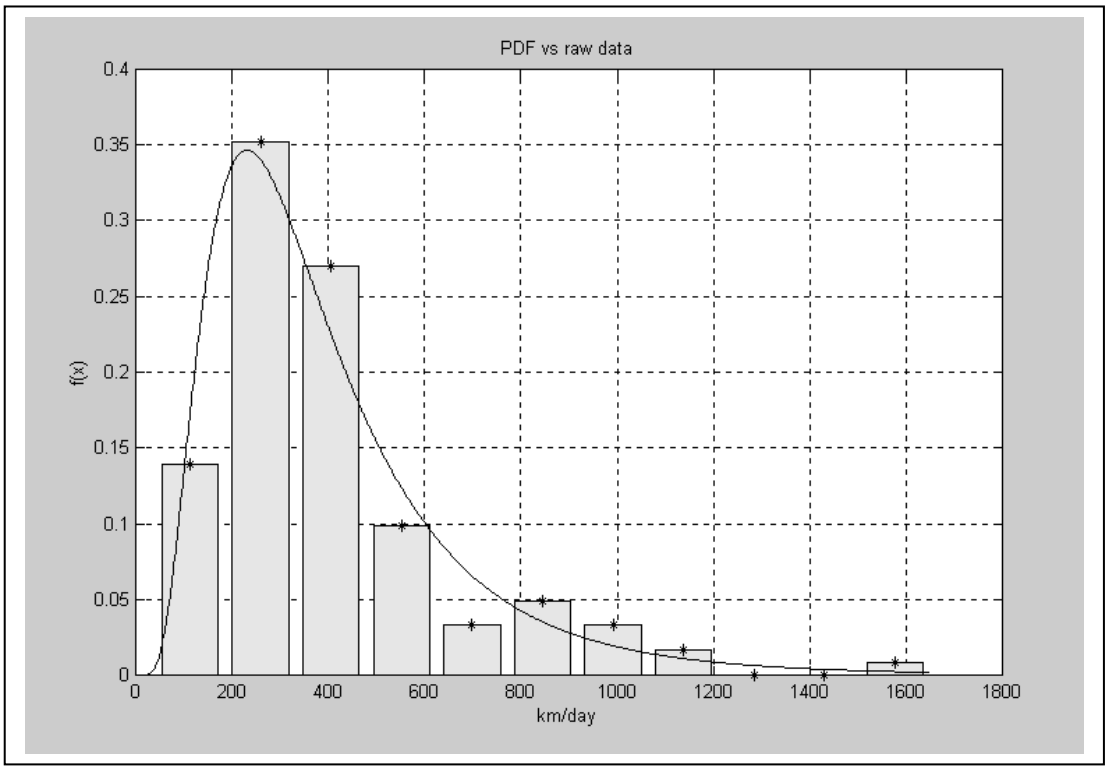

Figure 5-25 PDF of km/day versus raw data

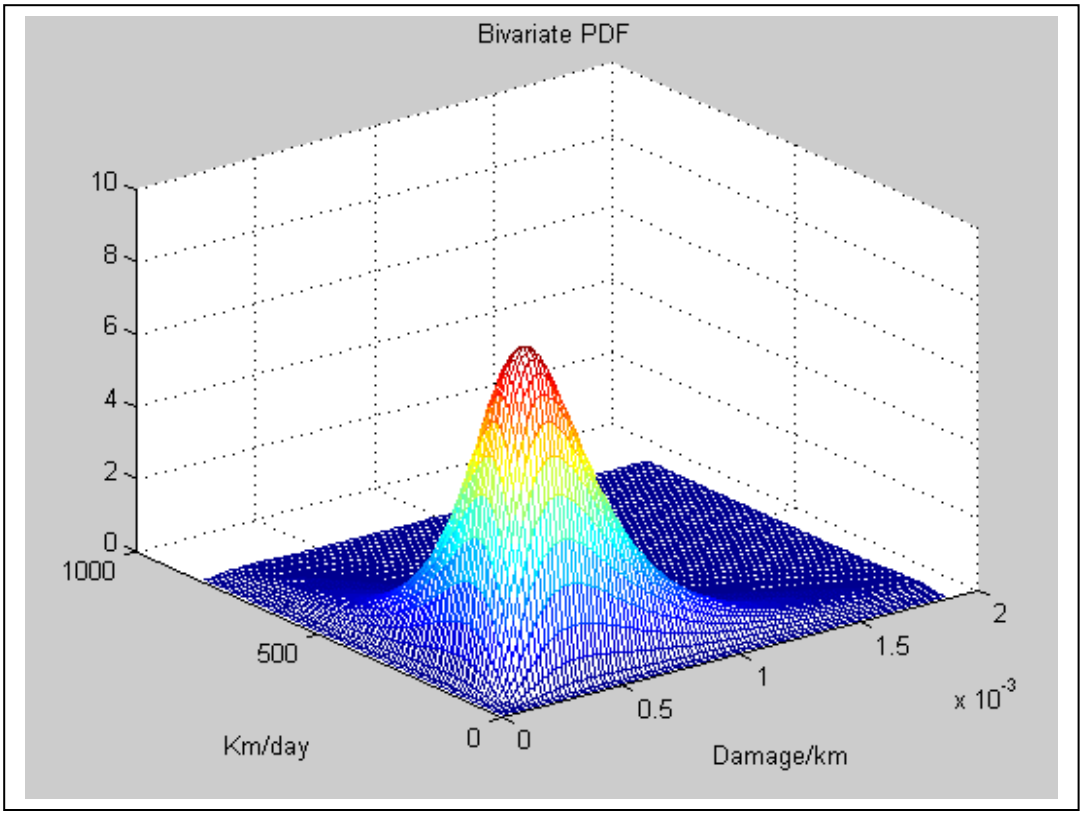

Figure 5-26 Bivariate distribution of km/day and D/km

5.5.4 Pick-up Truck

5.5.4.1 Fatigue processing

The measured data was downloaded onto computer and fatigue calculations were performed on each channel for each section of road. The damage was calculated using the same general material properties for all channels and road sections to obtain damage values that have no meaning in the absolute sense, but do give the relative severity between each road section for each channel. The damage for each road section was also divided by the distance to give a normalised damage per kilometre.

The damage per kilometre values for different road sections sampled for the usage profile and belonging to the same road category, were averaged to yield a single damage per kilometre value per channel per category. The results of these calculations are listed in Table 5-3.

Table 5-3: Damage/kilometre values for different road sections

Channel Description	Rural good Tar	Rural bad tar	Urban	Mountainous and winding	Good gravel	Bad gravel
Left front coil	2.73×10^{-8}	1.50×10^{-8}	1.60×10^{-7}	1.13×10^{-7}	2.70×10^{-7}	1.50×10^{-6}
Right front coil	3.75×10^{-8}	3.00×10^{-8}	2.20×10^{-7}	1.50×10^{-7}	4.40×10^{-7}	2.00×10^{-6}
Right rear diff	4.79×10^{-9}	2.30×10^{-9}	3.10×10^{-8}	1.10×10^{-8}	3.00×10^{-8}	1.50×10^{-7}
Left rear diff	5.30×10^{-9}	2.00×10^{-9}	2.10×10^{-8}	7.70×10^{-9}	3.40×10^{-8}	1.30×10^{-7}
Left front strut	2.50×10^{-10}	2.80×10^{-10}	1.30×10^{-9}	3.60×10^{-10}	2.00×10^{-9}	9.80×10^{-9}
Right front beam	5.90×10^{-9}	6.60×10^{-9}	3.00×10^{-8}	1.90×10^{-8}	3.10×10^{-7}	1.55×10^{-6}
Left beam centre	1.60×10^{-9}	2.80×10^{-9}	3.40×10^{-8}	1.00×10^{-8}	3.70×10^{-8}	2.20×10^{-7}
Round crossmem.	3.90×10^{-10}	8.20×10^{-11}	5.80×10^{-10}	5.50×10^{-10}	4.60×10^{-9}	2.60×10^{-8}
Left top door	3.50×10^{-10}	1.50×10^{-10}	6.10×10^{-10}	5.80×10^{-10}	6.60×10^{-9}	3.30×10^{-8}
Box left rear panel	3.40×10^{-10}	1.20×10^{-10}	1.80×10^{-10}	5.70×10^{-10}	1.33×10^{-10}	9.10×10^{-10}

The above results clearly show the relative severities of each category of road per channel. Comparisons of damage results between channels have no meaning (the damage on a coil spring and at a certain position on a differential are not comparable). A discrepancy concerning the relative damage calculated for the rural good surfaced category compared to the rural bad surfaced category can be observed. This may be ascribed to the subjective categorisation performed during the measurements.

5.5.4.2 Statistical processing of questionnaire data

A similar process to that described in paragraph 5.5.3.2 above for the minibus was followed for the pick-up truck. Eq. 5-21 was used to calculate the two parameters (km/month and damage/km). Lognormal probability density functions were fitted according to Eq. 5-22 and Eq. 5-23. The achieved fits are depicted in Figure 5-27 and Figure 5-28 below. These plots are for the average of channels 3 and 4, (left and right rear diff), which is indicative of the vertical loading on the rear axle. The same calculation can be done for any channel, but is shown here due to the fact that rear suspension leaf spring failures occurred on the vehicle during the durability testing. Again statistical dependence of the variables were assumed, implying the use of the bivariate distribution of Eq. 5-24.

From the questionnaire data it was found that the following distribution of cargo carrying could be assumed:
No load = 50%, Full load = 28%, Overload = 22%

The above results were used to compile test requirements and to perform failure prediction, as described in the next section.

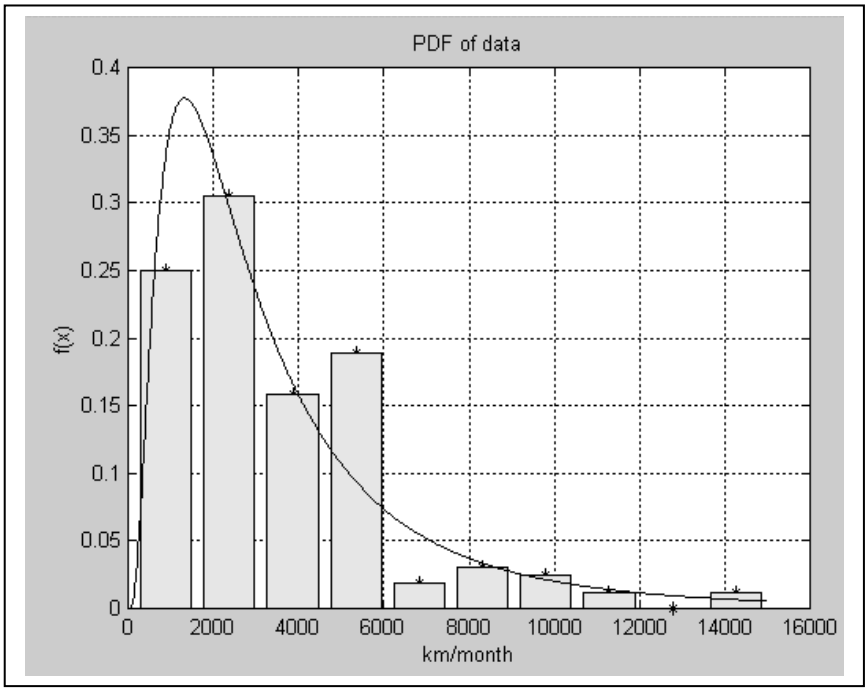

Figure 5-27 PDF of km/month vs raw data

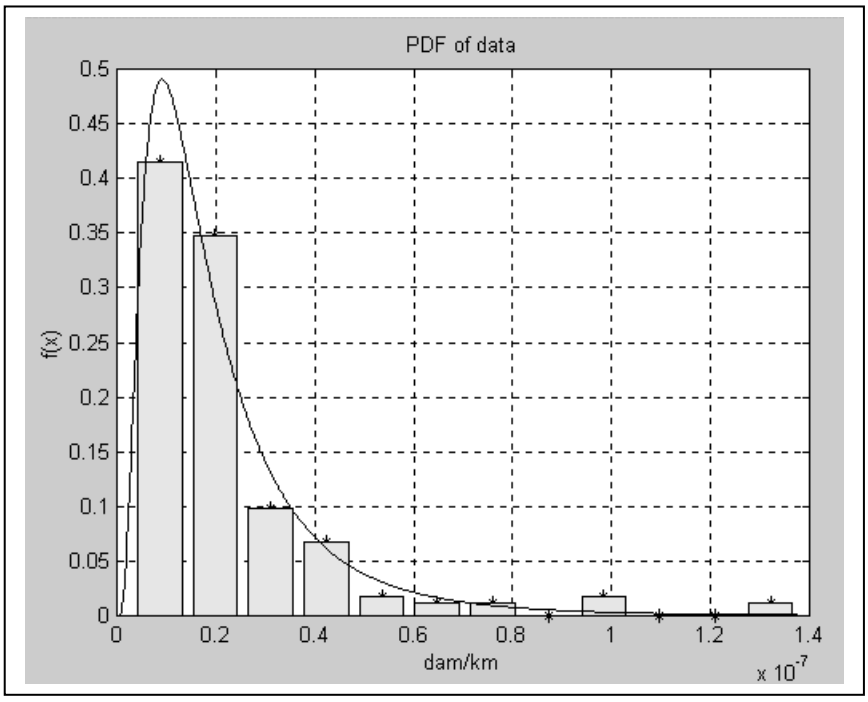

Figure 5-28 PDF of D/km versus raw data

5.6 TESTING REQUIREMENTS

5.6.1 General

In some instances, requirements, as derived from input loading determination, will be the same for design and testing. Representative dynamic loads could be used in dynamic finite element analysis, as well as for dynamic rig testing. Fatigue equivalent loads could be applied as sine wave, single amplitude loading in a test. Mostly, however, different requirements are set for testing, to what was used for the design. A physical test on a test track or a road simulator laboratory rig will apply load sequences that are of too long durations to be simulated by dynamic finite element analyses.

In this section, the derivation of testing requirements for the light commercial vehicles, as well as the ISO tank container, are dealt with.

5.6.2 Minibus

Although some aspects would require more detailed assessment, it was proposed that the statistical and fatigue presentation of the operational conditions which minibus taxi vehicles are subjected to, may be considered to be fairly accurate. Additionally, the methodology facilitates an extremely versatile means of deriving durability testing requirements.

Durability test requirements are established according to a target set by company policy. If this target is set in terms of distance without failure, the following method can be used to derive the appropriate durability requirement.

It is firstly necessary to also target a percentage users to be catered for, being defined as the percentage of vehicles which would reach the target distance without failure. The durability requirement will be set as a number of cycles to be completed on the test track without failure. The number of cycles implies a certain damage (D_{tt}). The required damage to be induced on the test track divided by the target distance without failure implies a vertical line on the D/km, km/day plane. D_{tt} should be chosen such that the percentage of the volume to the left of the straight line and underneath the surface defined by the 2-D PDF, would be larger than the target percentage users. Figure 5-29 depicts the results of such an analysis. Lines of different target distances are plotted on a plane of percentage users vs required cycles on the test track. As an example, if a target distance of 150 000 km without failure is set together with a percentage users of 96 %, the required number of cycles to be completed without failure on the test track may be read off as 10 000.

This result may also be presented in terms of a graph of percentage users vs required severity ratio (refer to Figure 5-30). This graph may be used to read off the required severity ratio for a certain percentage users (e.g. 7.6:1 at 95 %, implying that for every 1 kilometre on the test track, 7.6 kilometres of normal use, pertaining to 95 % of the users, will be simulated).

Similarly, if the company policy requires a target to be set in terms of years without failure (e.g. warranty period), the following procedure is followed:

Again a corresponding percentage users to be catered for must be set. The required damage to be induced by the test track (D_{tt}, which is related to the number of cycles on the test track) divided by the number of days without failure implies a hyperbola on the D/km,

km/day plane. D_{tt} must be chosen such that the percentage volume below this hyperbola and underneath the 2-D PDF, is more than the percentage users. Figure 5-31 depicts the results of such an analysis. Lines of different years without failure are plotted on a "cycles on test track" versus "percentage users" plane. As an example, a target of 10 years without failure for a percentage users of 95 % would require 30 000 cycles to be performed on the test track without failure.

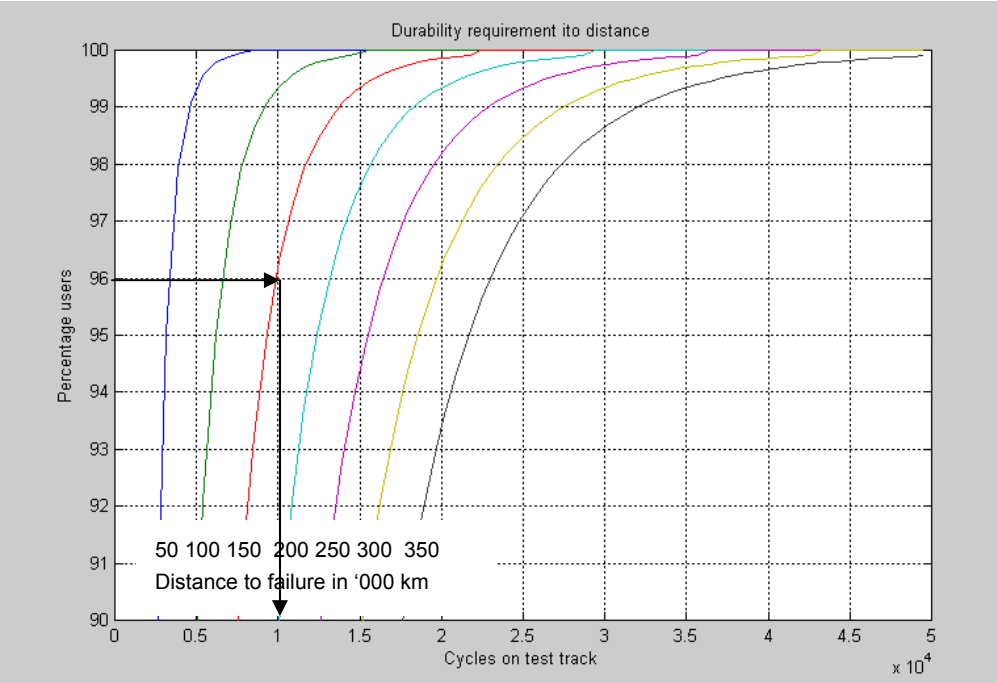

Figure 5-29 Durability requirements ito distance

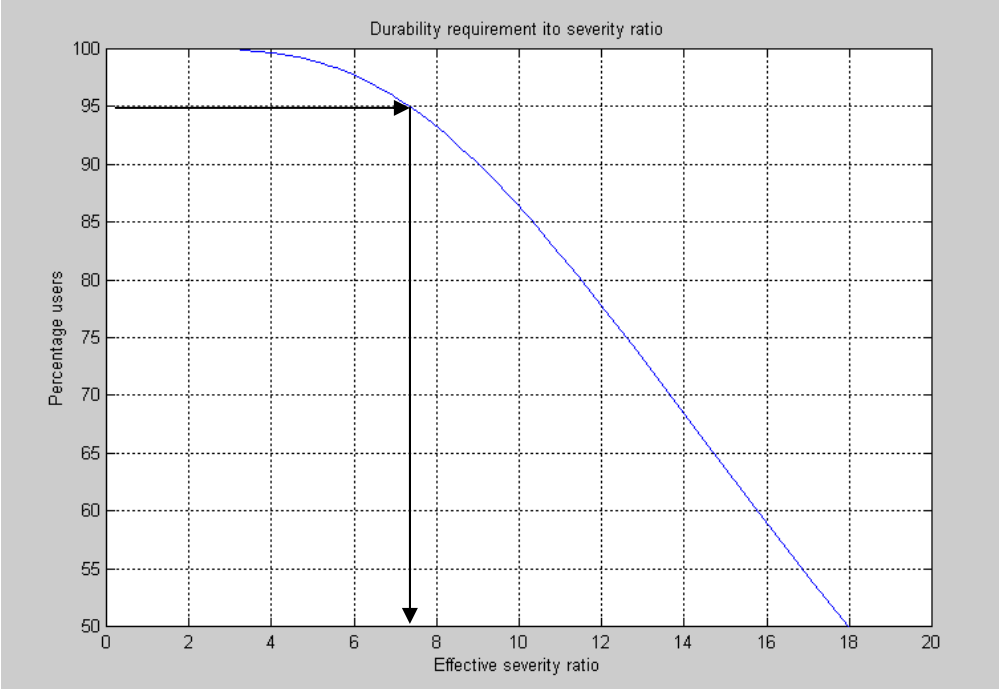

Figure 5-30 Durability requirements ito severity ratio

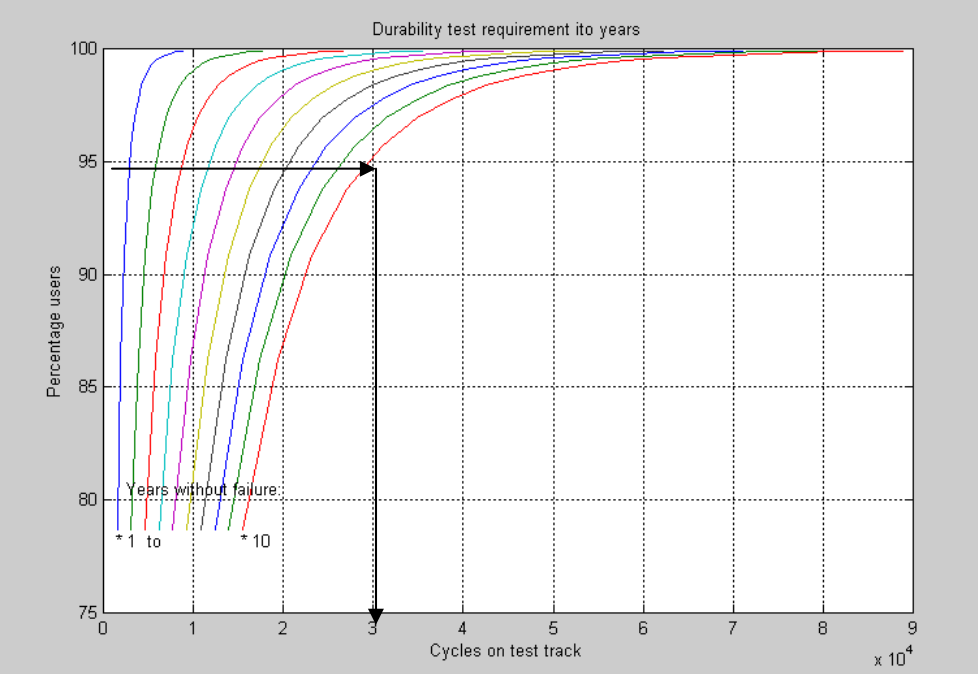

Figure 5-31 Durability requirement in terms of years

5.6.3 Pick-up Truck

5.6.3.1 Compilation of laboratory test sequence

From the fatigue damage calculations, only certain sections of the measured roads were selected to be simulated in the laboratory. This was necessary in order to equally accelerate the laboratory test for all channels by selectively replacing less severe road sections with more severe road sections. For this purpose the fatigue damages per unit time for each measured field file per channel were calculated

From this information, a laboratory durability sequence was compiled, utilising the measured field files with the highest damage per unit time. In order to achieve a similar test acceleration factor for all strain channels, it was necessary to find the right mix of field files and repetitions. This is achieved in a trial-and-error process. The solution would not be unique.

5.6.3.2 Monte Carlo establishment of durability test requirement

A process somewhat different to that followed for the minibus, but with the same aim, was used. It was decided to use the Monte Carlo approach, rather than an analytical approach, since it would then be possible to treat further parameters, such as the damage to failure, as well as the cargo loading, as statistical parameters. A flowchart of the process to establish 10 000 random samples of the parameters according to the distributions, is depicted in Figure 5-32.

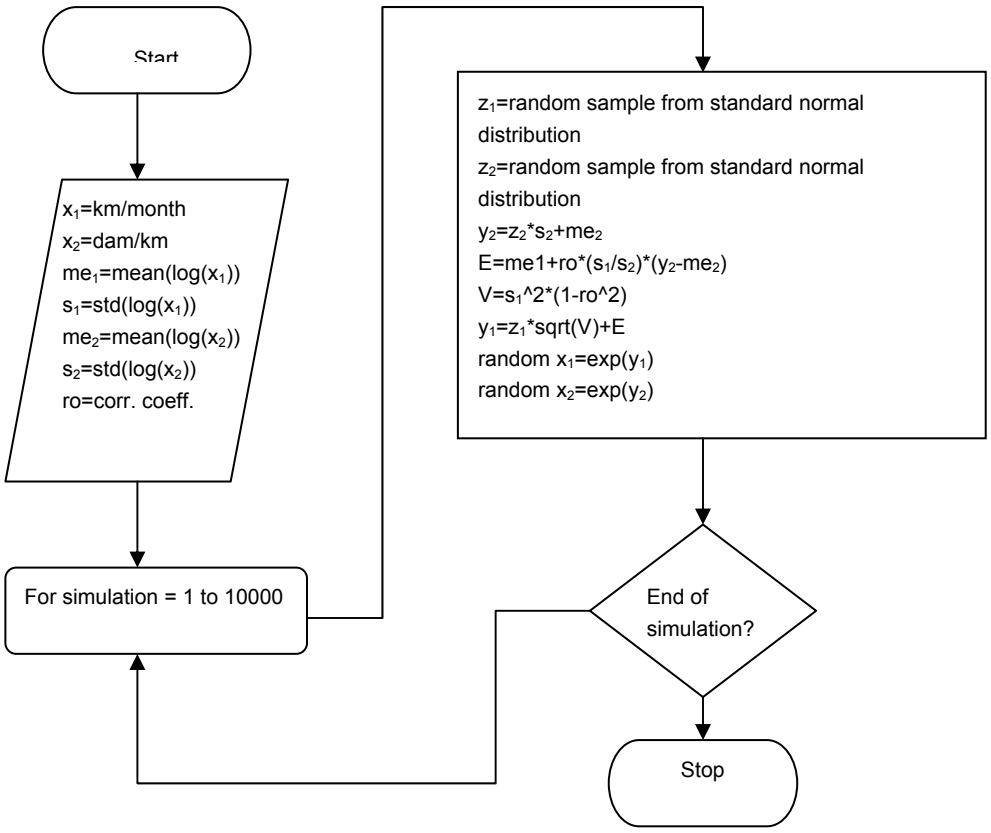

Figure 5-32 Monte Carlo process

Measurements with different cargo loads indicated that the damage reduces by a factor 0.4 for the no load case and increases with a factor 1.4 for the 20 % overload case. For each of the x_2 [D/km] samples these factors were applied, based on a uniformly distributed random number between 0 and 1 (if between 0 and 0.5 – multiply by 0.4, if between 0.78 and 1, multiply by 1.4). This shows the strength of the Monte Carlo method.

The 10 000 random samples of x_2 are then sorted from small to large and when plotted against it's index/10 000×100, yields a cumulative distribution function (refer to Figure 5-33).

The damage induced on the rear axle channels when applying the test sequence, was 7.9×10^{-6} per test cycle. If a target of 300 000 failure free kilometres are set for the vehicle, the number of cycles required from the testing can be calculated as 300 000 $\times$ x_2/damage per cycle. If the sorted 10 000 random samples of x_2 are used in this calculation and the result is plotted against the index/10 000×100, the required number of test cycles to achieve 300 000 km of usage is exhibited as a function of the percentage users (refer to Figure 5-34).

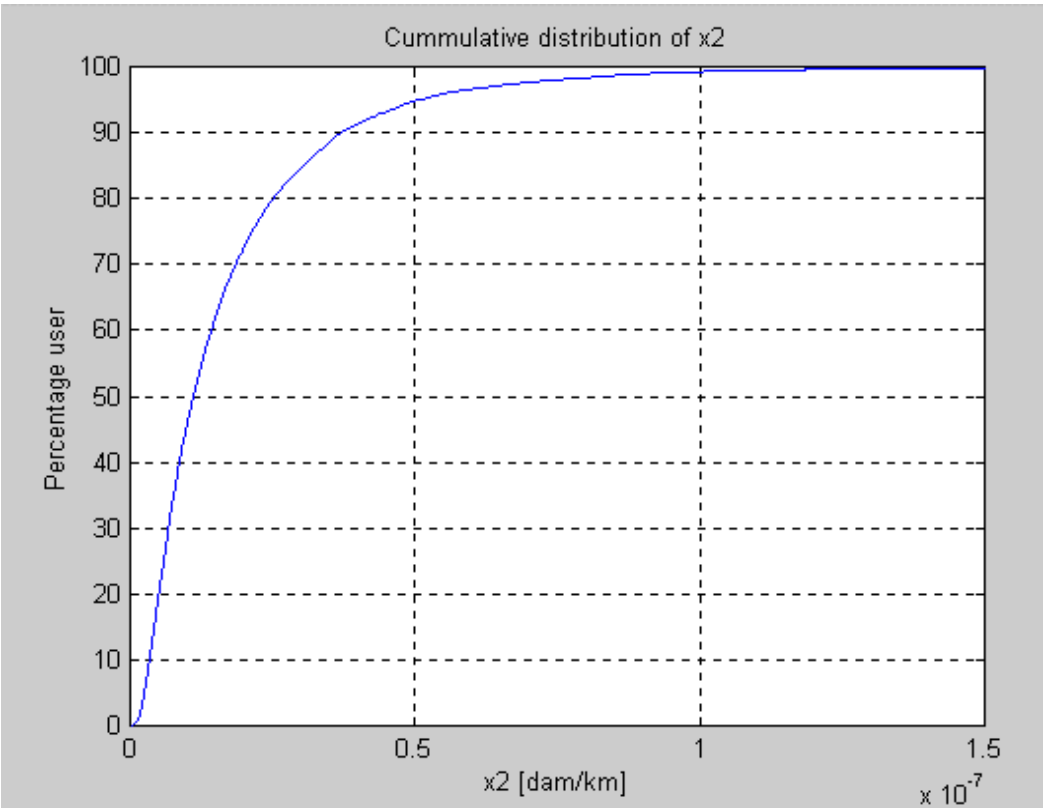

Figure 5-33 Cumulative distribution of x_2

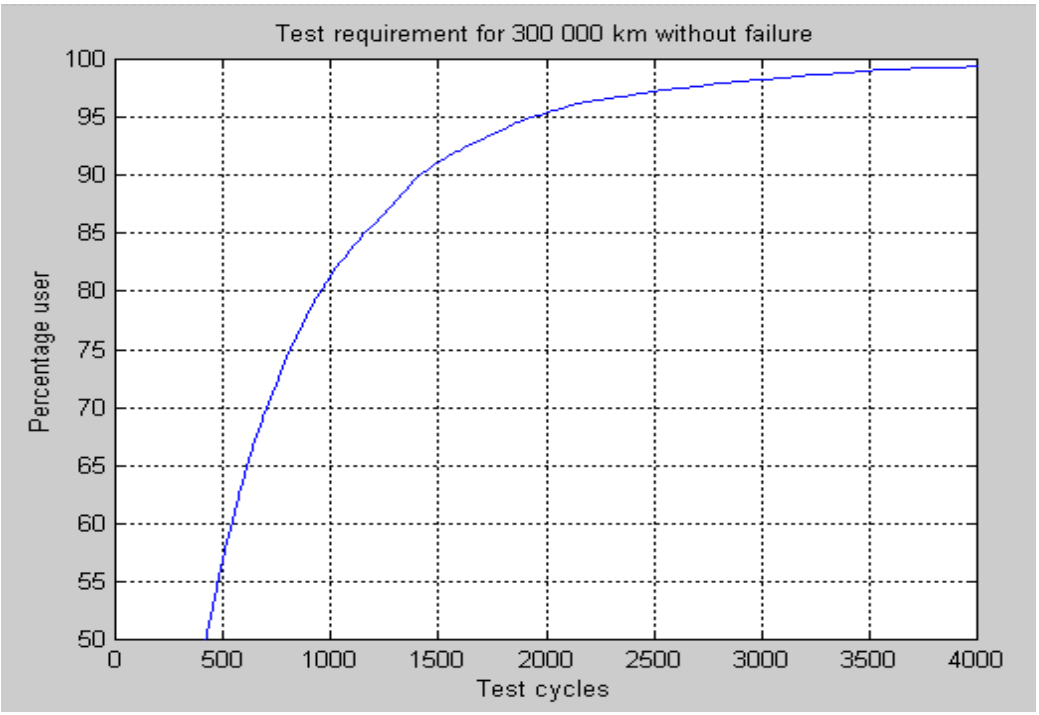

Figure 5-34 Test requirement for 300 00 km without failure

From Figure 5-34, the number of test cycles required to achieve 300 000 km of usage for any percentage of users can be determined. 2000 cycles are required if 300 000 km for 95 % of the users are to be achieved (only 5 % of users would induce more damage in 300 000 km). The duration of one test cycle was approximately one hour, which implied that at 24 hours per day and 7 days per week, the test would be completed in 3 months. At 300 000 km in 2000 hours, the effective simulation speed for the 95 % user would be 150 km/h. For the 50 % user, an additional acceleration of 2000/450 = 4.44 is achieved, implying an effective test speed of 666 km/h.

The testing performed according to the above criteria, as well as the failure predictions performed, based on the test results, are described in 6.2.3.

5.6.4 ISO Tank Container

Testing on the ISO tank container was performed on a servo-hydraulic test rig. In this instance, the requirements derived for fatigue design were also used for testing. The fatigue equivalent loads were used as inputs on the rig as sine waves. Care was taken to avoid frequencies at which resonant dynamics are excited.

A very important inadequacy of the testing method was that it was not practically possible to perform the testing whilst applying the vertical, longitudinal, lateral and pitching loads simultaneously, as is theoretically required to simulate the correct damage in all areas of the structure. The different loads were therefore applied in a series of tests. It was argued and substantiated through finite element analysis, that most of the critical areas were each only sensitive to one of the load directions. For those areas sensitive to more than one load affected the stresses, corrections were made to the results, taking into account the reduced stresses due to the loss of the combined effects and the increased number of cycles (2 million for each load).

5.7 CLOSURE

In this chapter, comprehensive techniques for deriving input loading requirements for design and testing, were demonstrated. As an alternative for performing dynamic finite element analyses, robust methods were presented to derive fatigue equivalent loads, applied in static finite element analyses, or single amplitude rig tests.

For test track or road simulator laboratory tests, powerful methods to establish testing requirements based on statistical targets, were developed.

In the next chapter, fatigue assessment and correlation of the results obtained in this chapter, are dealt with.